Argonne
NATIONAL LABORATORY

... for a brighter future

U.S. Department of Energy

THE UNIVERSITY OF CHICAGO

Office of Science
U.S. DEPARTMENT OF ENERGY

A U.S. Department of Energy laboratory managed by The University of Chicago

Advanced Methods for Transport Simulation

Paul Fischer
Misun Min
James Lottes
Chaman Verma

AMR Meeting, LLNL, May 22-24, 2007

Objectives: Advanced Methods for Transport Simulation

- *Focus:*
  - *High-order methods for challenging DOE science and engineering applications*
  - *State-of-the-art iterative solvers*
  - *Deployment to petascale architectures, $P > 10^6$ (algorithms <u>and</u> software)*
  - *Test and develop through extensive interactions with DOE and university collaborators on cutting-edge science problems*

SEM-based simulation of magneto-rotational instability. P=32K BGW Simulation. Obabko, Cattaneo, Fischer.

Outline

Provide a quick overview of advances/concerns in

- scalability
- accuracy
- stability
- solvers

for convective transport problems with examples interwoven throughout.

Algorithms & Software: Targeting 1 Million Processors

- Algorithmically:
  - Minimally dispersive discetizations: high-order, high accuracy per pt.
    - *Important for long-time integrations undertaken at Petascale*
  - Scalable iterative solvers:
    - *Schwarz/MG preconditioners*
    - *Low communication parallel coarse grid solvers (all-to-all in sublinear complexity)*
- Architecturally (*where software meets reality*)
  - No P^2 storage *(i.e., no P-sized arrays per proc.)*
  - No P^2 anything
  - locally structured data *SEM → N x N x N sized blocks*
  - use BLAS3 wherever possible *favorable work/data-access ratio*
  - quad data alignment for "*instruction-issue*" challenged processors
    - *e.g., early Weitek chips, Intel i860, BGL double hummer, … more in future*
  - *etc. etc.*

A high-order example: Spectral Element Method

(Patera 84, Maday & Patera 89)

- Variational method, similar to FEM, using *GL* quadrature.
- Domain partitioned into E high-order quadrilateral (or hexahedral) elements (decomposition may be nonconforming - *localized refinement*)
- Trial and test functions represented as N th-order tensor-product polynomials within each element. (N ~ 4 -- 15, typ.)
- EN^3 gridpoints in 3D, EN^2 gridpoints in 2D.
- Converges *exponentially fast* with N for smooth solutions.

3D nonconforming mesh for
arterio-venous graft simulations:
E = *6168* elements, N = *7*

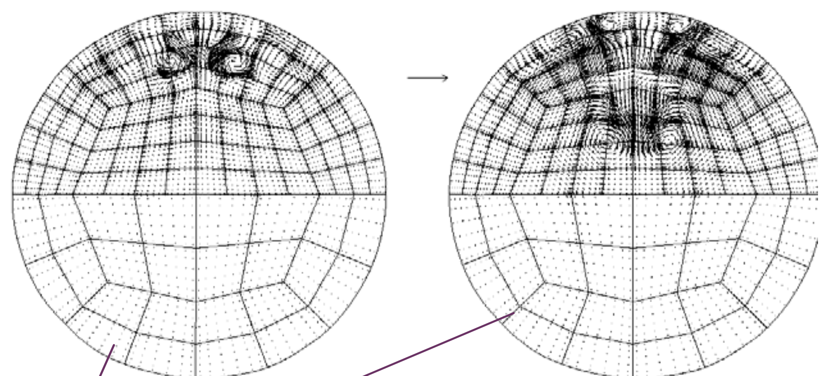

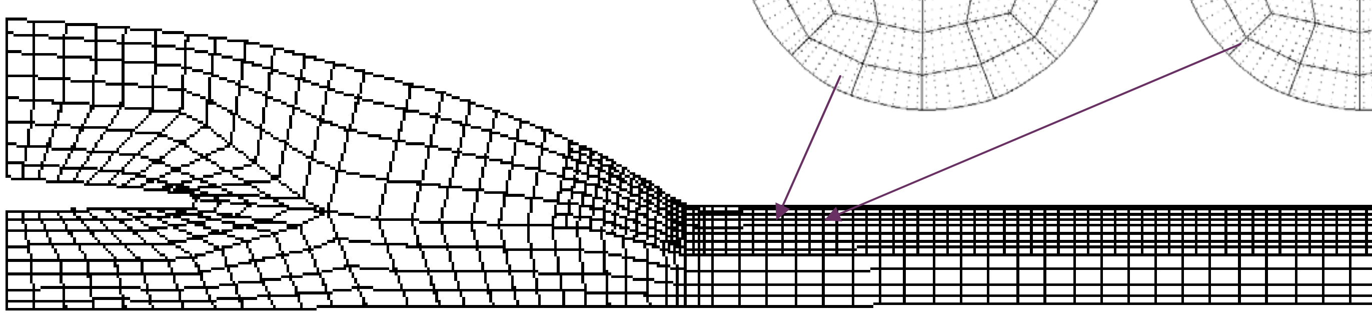

Accuracy & Cost

Spectral Element Convergence:

Exponential for smooth solutions:

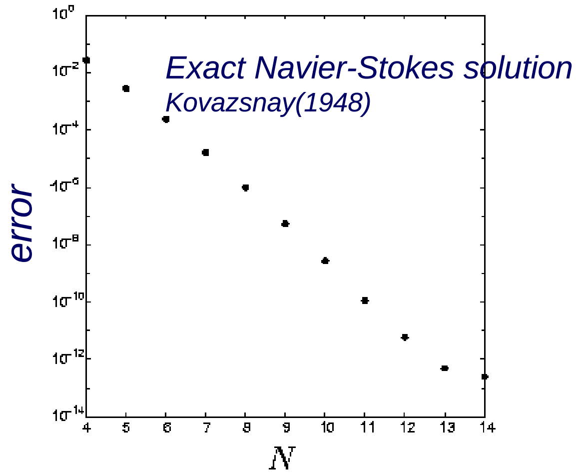

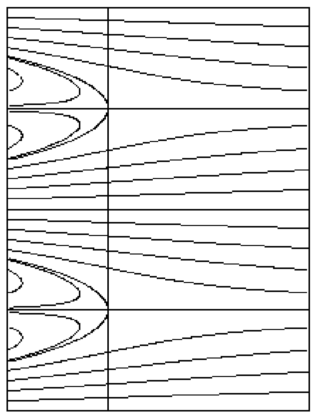

For nonsmooth (e.g., under-resolved) problems, good transport achieved because resolved modes are propagated accurately.

Can show that most of the benefit is realized with N ~ 8-16.

Key is to have a stable formulation.

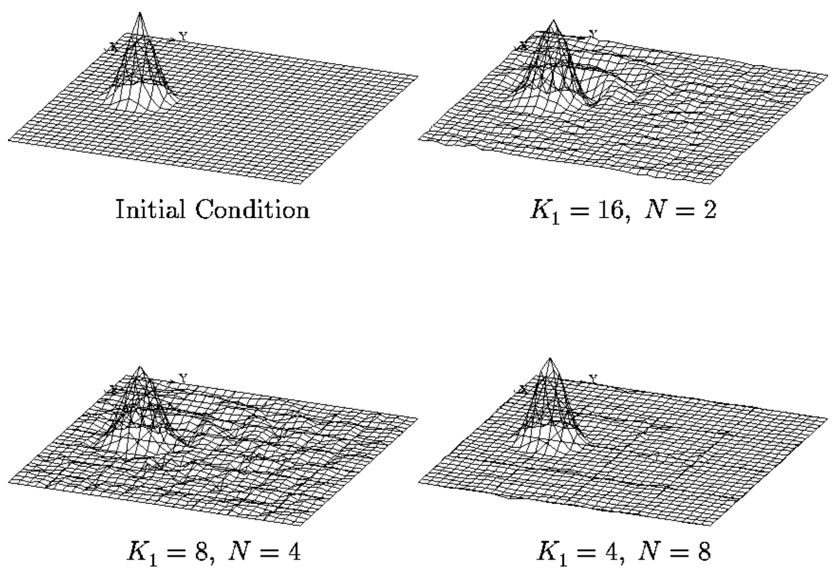

32x32 grid convection of pointed cone

Model Problem: convection-diffusion $u_t + \mathbf{c} \cdot \nabla u = \nu \nabla^2 u$

Find $u \in X_0^N \subset H_0^1$ *such that*

$$(v, u_t)_N + (v, \mathbf{c} \cdot \nabla u)_M = \nu (\nabla v, \nabla u)_N \quad \forall v \in X_0^N,$$

- $(f, g)_M := \sum_{j=0}^{M} \rho_j^M f(\xi_j^M) g(\xi_j^M)$, $\quad$ (1-D, $\Omega = [-1, 1]$)
- ξ_j^M, ρ_j^M—Mth-order Gauss-Legendre points, weights.

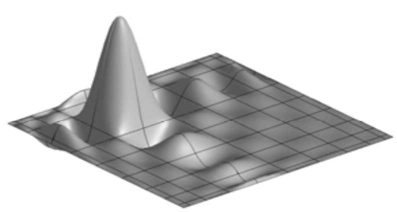

2D basis function, N=10

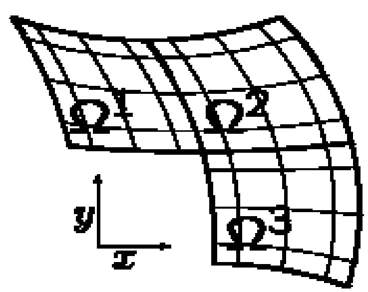

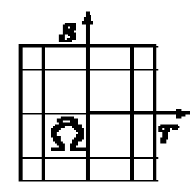

E=3, N=4

Fast Operator Evaluation

- *Local tensor-product form* (2D),

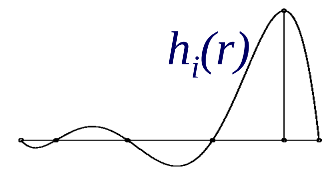

$$u(r,s) = \sum_{i=0}^{N}\sum_{j=0}^{N} u_{ij}\, h_i(r)\, h_j(s), \qquad h_i(\xi_p) = \delta_{ip}, \;\; h_i \in \mathbf{P}_N$$

allows derivatives to be evaluated as matrix-matrix products:

$$\left.\frac{\partial u}{\partial r}\right|_{\xi_i,\xi_j} = \sum_{p=0}^{N} u_{pj} \left.\frac{dh_p}{dr}\right|_{\xi_i} = \sum_p \underbrace{\hat{D}_{ip}\, u_{pj}}_{mxm} =: D_r \underline{u}$$

- *Work for SEM operators in 3D is reduced from O(N^6) to O(N^4)* *Orszag 80*
- *Data access requirements are equivalent to centered finite-differences*

Cost vs. Accuracy:

SE-DG method for Maxwell's equations: *Misun Min, ANL*

- *nanophotonics*
- *accelerator modeling*

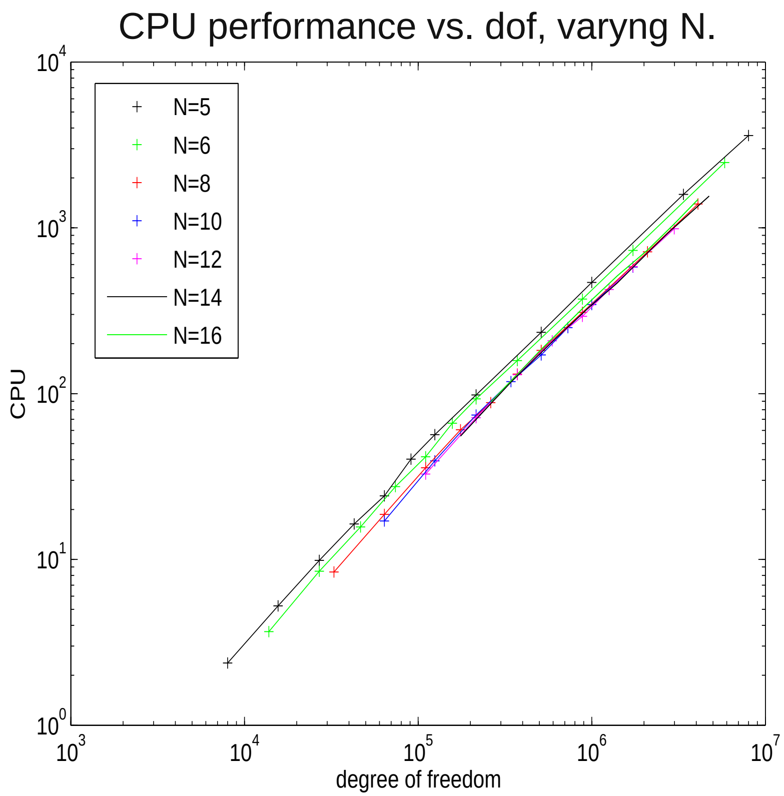

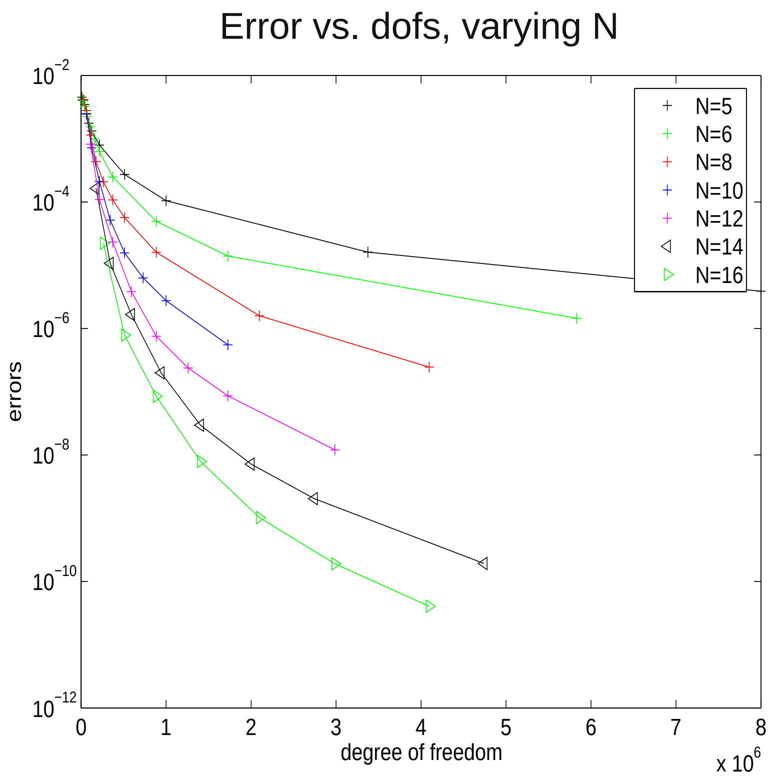

Periodic Box; 32 nodes, each with a 2.4 GHz Pentium Xeon

Stability

Filter-Based Stabilization

(Gottlieb et al., Don et al., Vandeven, Boyd, ...)

- *At end of each time step:*
  - Interpolate *u* onto GLL points for P_{N-1}
  - Interpolate back to GLL points for P_N

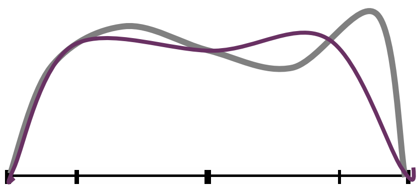

$$F_1(u) = I_{N-1}\, u$$

  - Results are smoother with linear combination: *(F. & Mullen 01)*

$$F_\alpha(u) = (1-\alpha)\, u + \alpha\, I_{N-1}\, u \qquad (\alpha \sim 0.05 - 0.2)$$

- *Post-processing — no change to existing solvers*
- *Preserves interelement continuity and spectral accuracy*
- *Equivalent to multiplying by (1-α) the Nth coefficient in the expansion*
  - $u(x) = \Sigma\, u_k\, \phi_k(x); \quad \phi_k(x) := L_k(x) - L_{k-2}(x)$ *(Boyd 98)*

Numerical Stability Test: Shear Layer Roll-Up

(Bell et al. JCP 89, Brown & Minion, JCP 95, F. & Mullen, CRAS 2001)

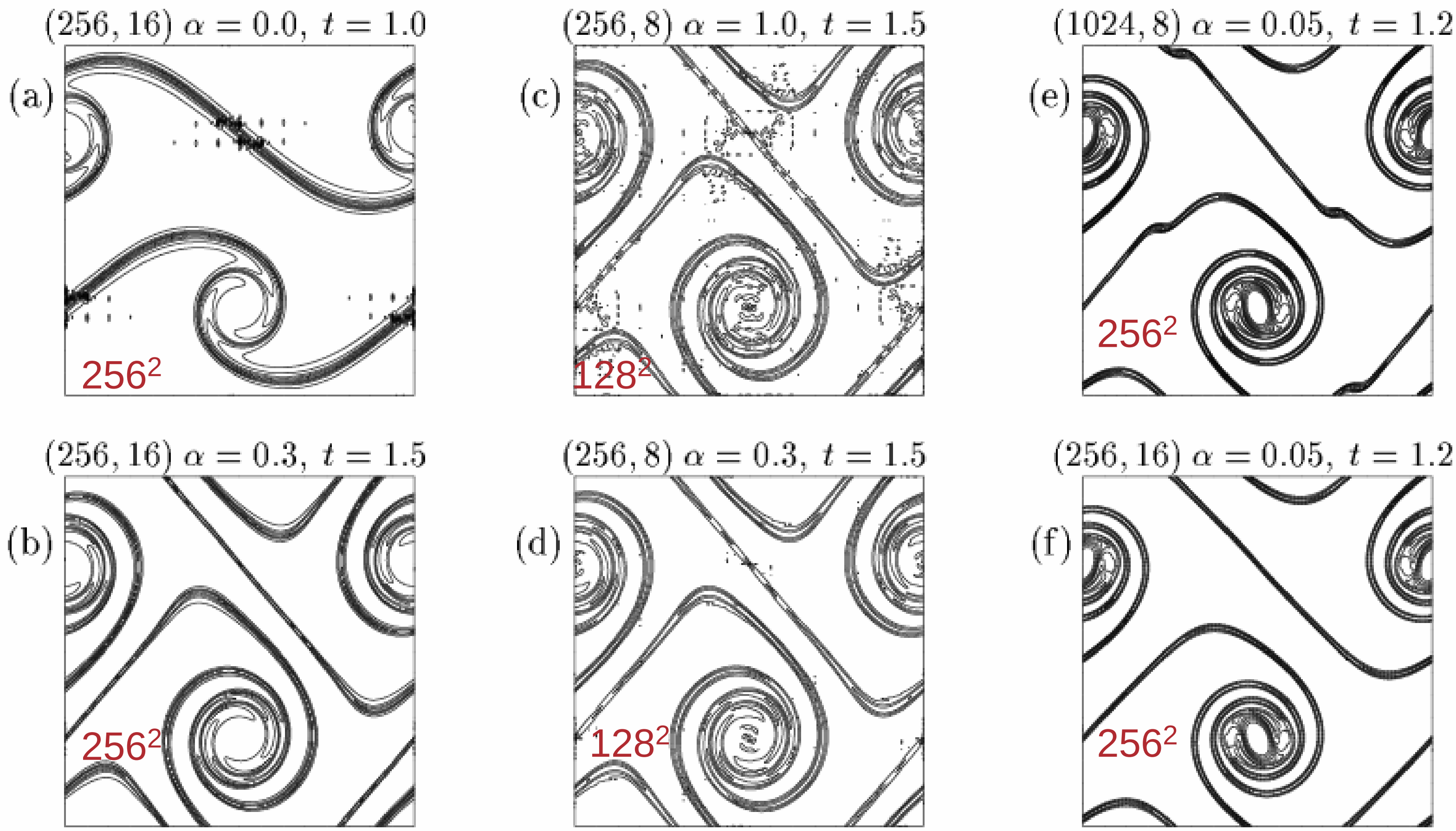

Figure 1: Vorticity for different (K, N) pairings: (a–d) $\rho = 30$, $Re = 10^5$, contours from -70 to 70 by 140/15; (e–f) $\rho = 100$, $Re = 40,000$, contours from -36 to 36 by 72/13. (cf. Fig. 3c in [4]).

Error in Predicted Growth Rate for Orr-Sommerfeld Problem at Re=7500

Spatial and Temporal Convergence *(FM, 2001)*

	$\Delta t = 0.003125$		$N = 17$	2nd Order		3rd Order	
N	$\alpha = 0.0$	$\alpha = 0.2$	Δt	$\alpha = 0.0$	$\alpha = 0.2$	$\alpha = 0.0$	$\alpha = 0.2$
7	0.23641	0.27450	0.20000	0.12621	0.12621	171.370	0.02066
9	0.00173	0.11929	0.10000	0.03465	0.03465	0.00267	0.00268
11	0.00455	0.01114	0.05000	0.00910	0.00911	161.134	0.00040
13	0.00004	0.00074	0.02500	0.00238	0.00238	1.04463	0.00012
15	0.00010	0.00017	0.01250	0.00065	0.00066	0.00008	0.00008

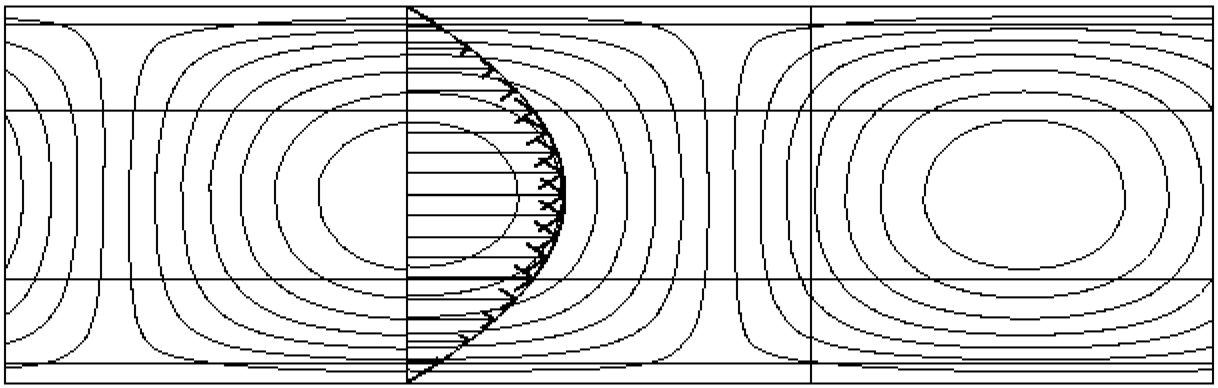

Base velocity profile and perturbation streamlines

Filtering provides a convergent path to resolving difficult flows.

Low-speed streaks and log-law velocity profiles for $Re=30{,}000$ simulation of turbulent flow in a reactor core coolant passage.

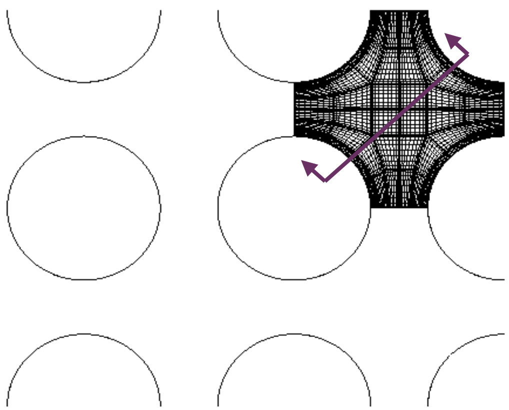

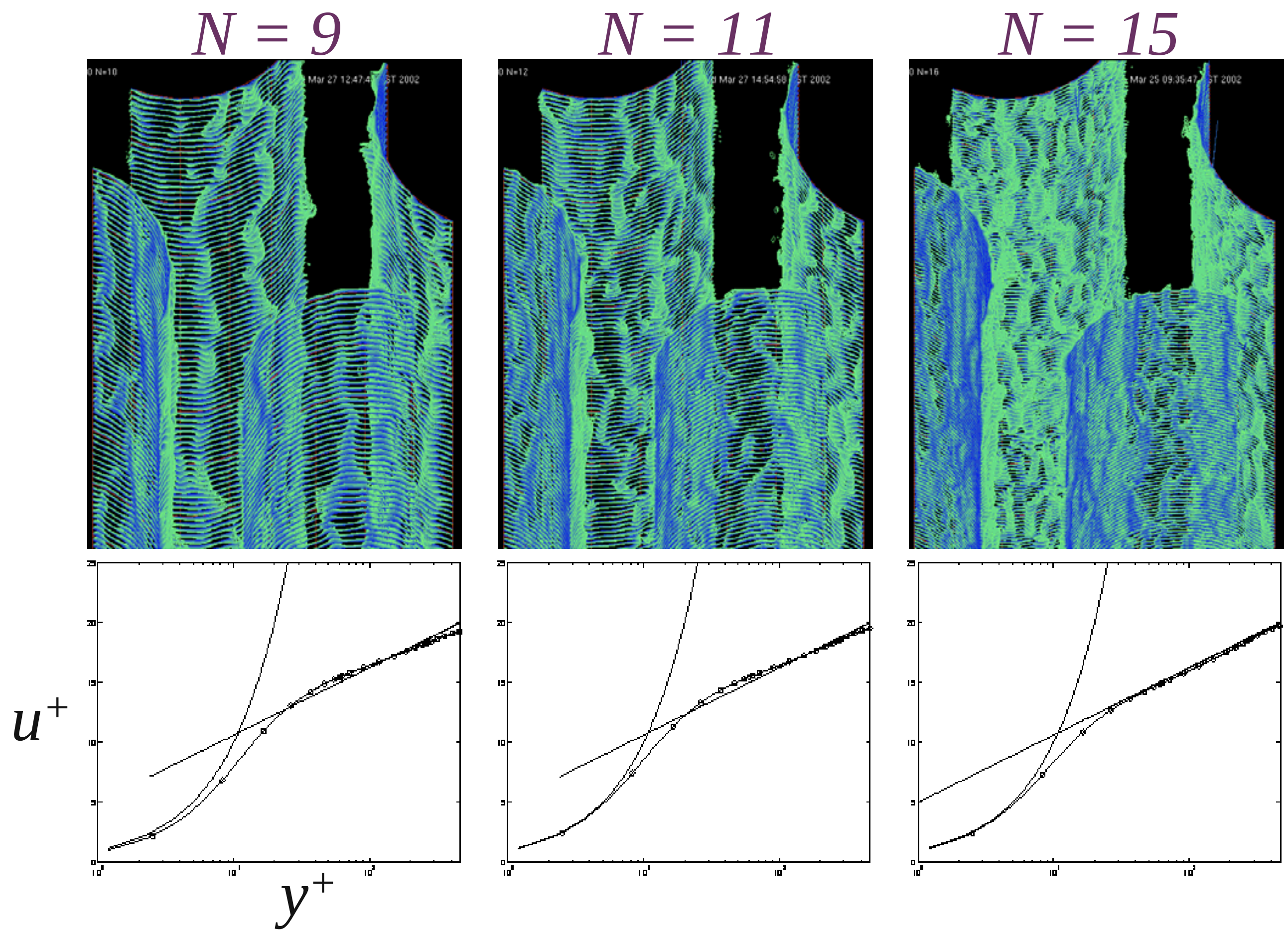

Rod Bundle Validation: Nek5000 Comparison w/ Experimental Data

(F. & Tzanos, 05)

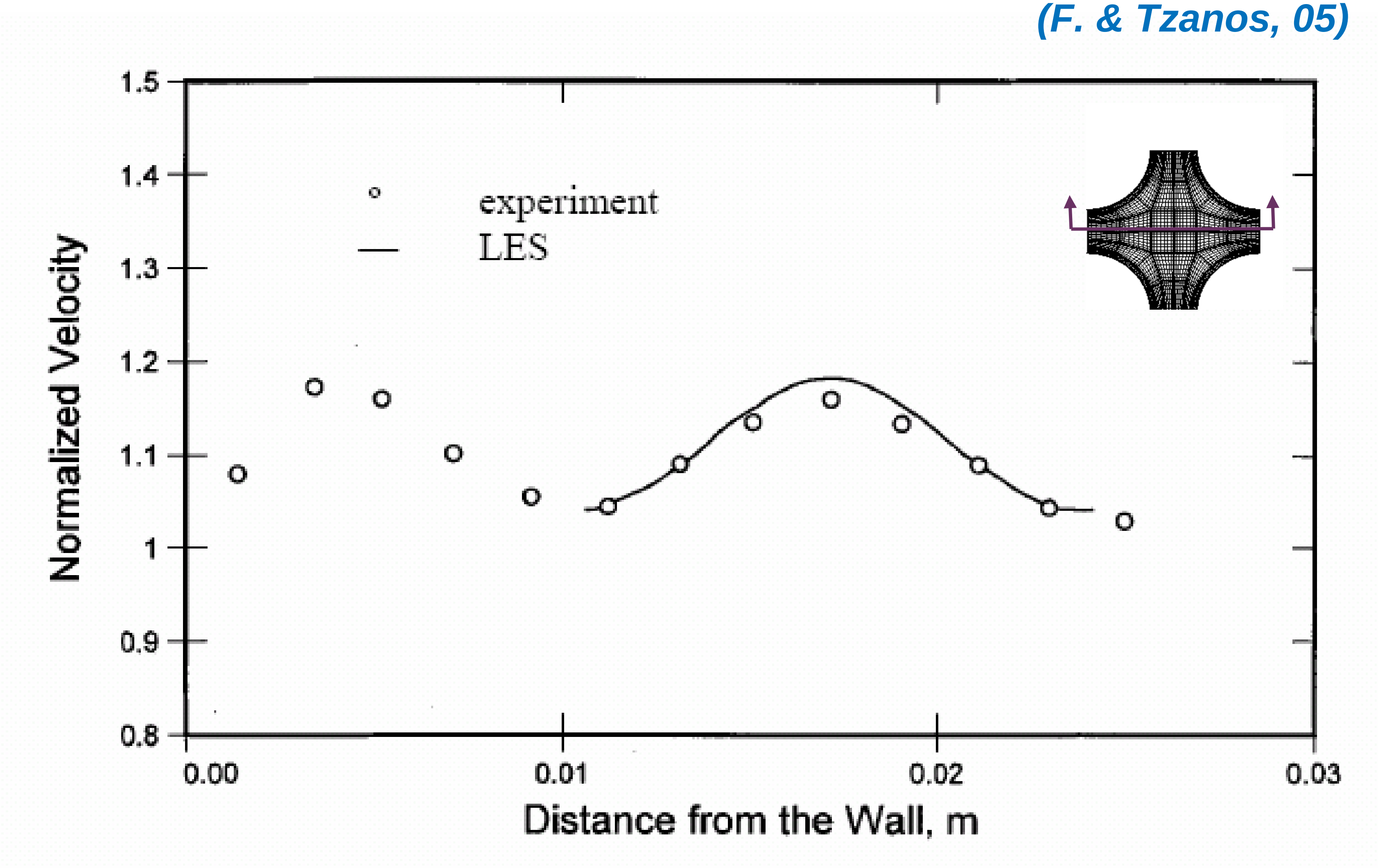

Why Does Filtering Work ?
(Or, Why Do the Unfiltered Equations Fail?)

Double shear layer example:

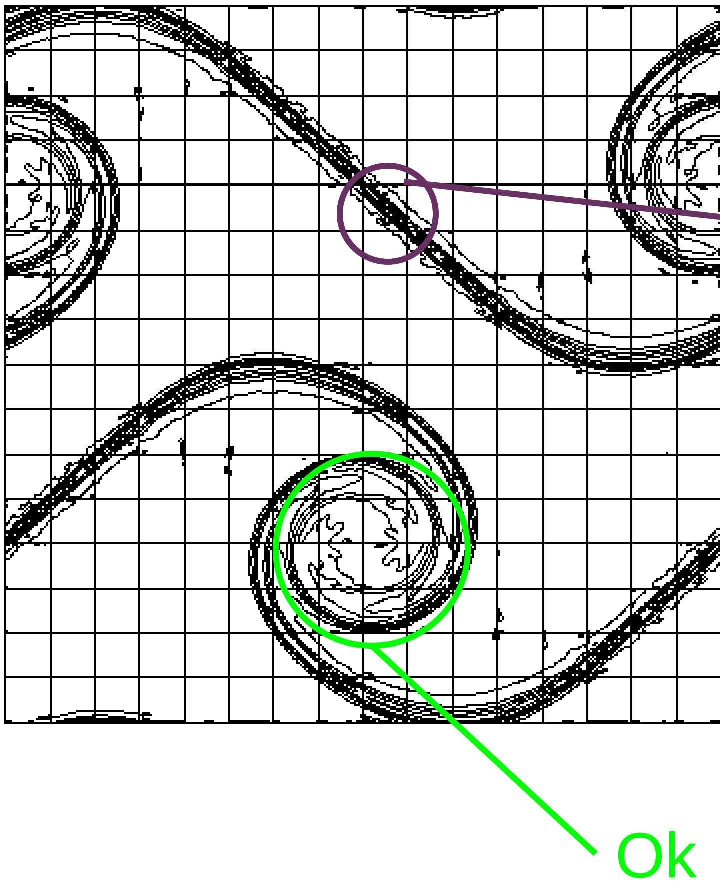

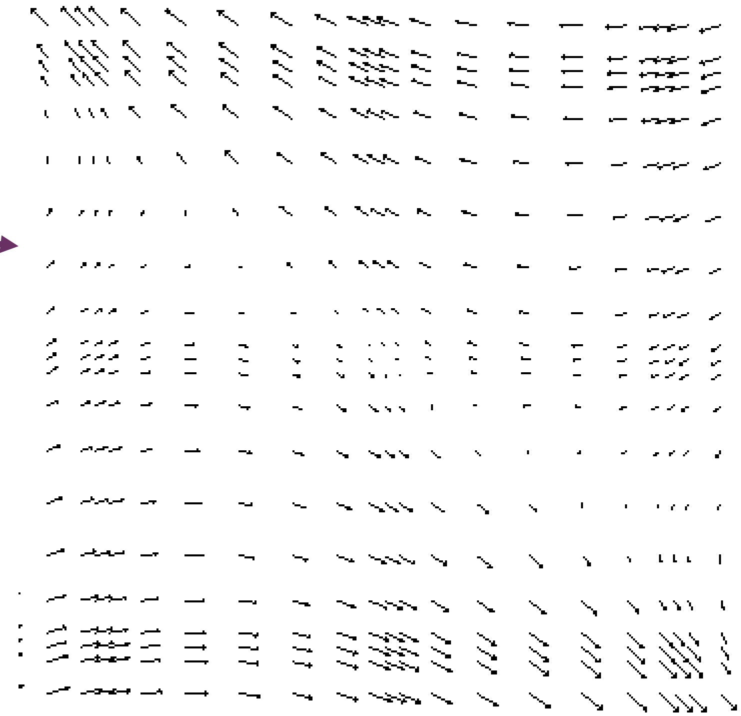

High-strain regions are troublesome…

Why Does Filtering Work ?
(Or, Why Do the Unfiltered Equations Fail?)

Consider the model problem: $$\frac{\partial u}{\partial t} = -\mathbf{c} \cdot \nabla u$$

Weighted residual formulation: $$B\frac{d\underline{u}}{dt} = -C\underline{u}$$

$$\begin{aligned}
B_{ij} &= \int_\Omega \phi_i \phi_j \, dV = \text{symm. pos. def.} \\
C_{ij} &= \int_\Omega \phi_i \, \mathbf{c} \cdot \nabla \phi_j \, dV \\
&= -\int_\Omega \phi_j \, \mathbf{c} \cdot \nabla \phi_i \, dV - \int_\Omega \phi_j \phi_j \nabla \cdot \mathbf{c} \, dV \\
&= \text{skew symmetric, if } \nabla \cdot \mathbf{c} \equiv 0. \\
\longrightarrow B^{-1}C &= \text{skew symmetric}
\end{aligned}$$

Discrete problem should never blow up.

Why Does Filtering Work ?
(Or, Why Do the Unfiltered Equations Fail?)

Weighted residual formulation vs. spectral element method:

$$C_{ij} \;=(\phi_i, \mathbf{c}\cdot\nabla\phi_j) = \; -C_{ji}$$

$$\tilde{C}_{ij} \;=(\phi_i, \mathbf{c}\cdot\nabla\phi_j)_N \neq \; -\tilde{C}_{ji}$$

This suggests the use of over-integration (dealiasing) to ensure that skew-symmetry is retained

$$C_{ij} \;=\; (J\phi_i, (J\mathbf{c})\cdot J\nabla\phi_j)_M$$

$$J_{pq} \;:=\; h_q^N(\xi_p^M) \quad \text{interpolation matrix (1D, single element)}$$

Aliased / Dealiased Eigenvalues: $u_t + \mathbf{c} \cdot \nabla u = 0$

- Velocity fields model first-order terms in expansion of straining and rotating flows.
  - Filtering / dealiasing attacks the leading unstable mode in straining field.
  - Rotational case is skew-symmetric.

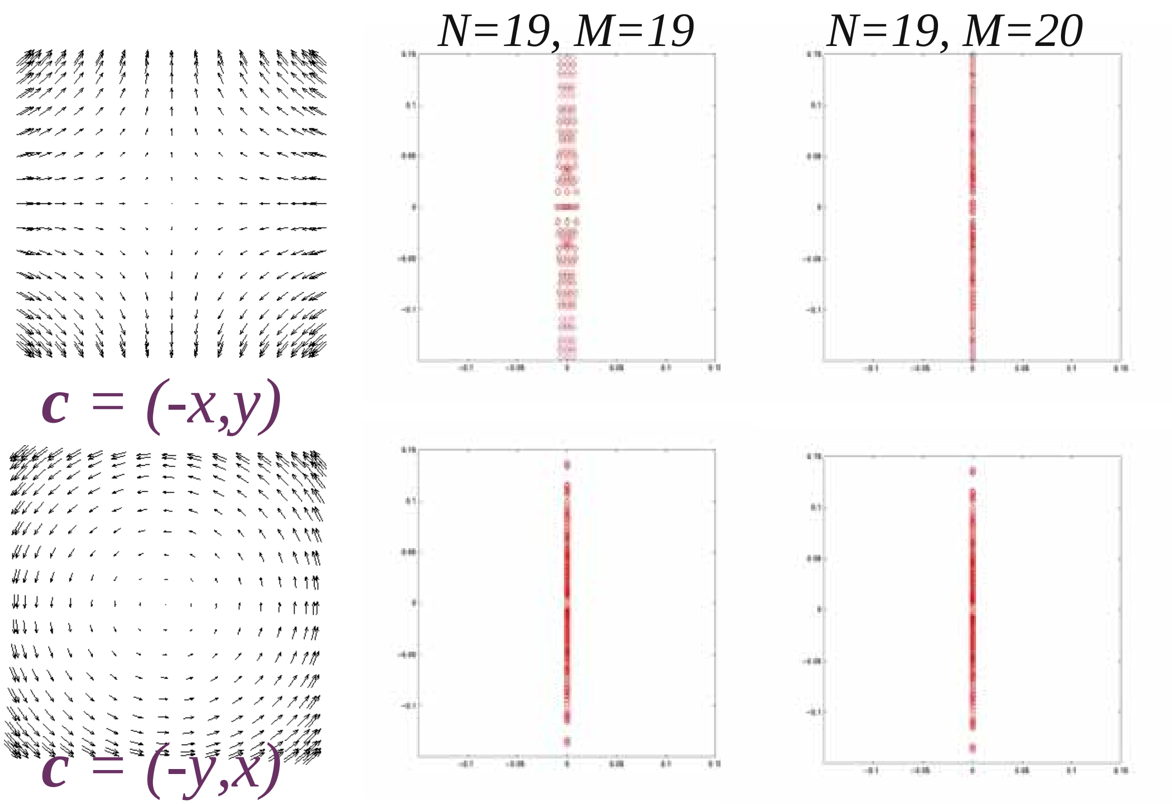

Solvers

- Incompressible Navier-Stokes equations imply a Poisson-like solve at each time step to impose divergence-free constraint.
- This solve is the leading-order computational bottleneck.

Two-Level Overlapping Additive Schwarz Preconditioner

(Dryja & Widlund 87, Pahl 93, PF 97, FMT 00)

$$\underline{z} = M\underline{r} = \sum_{e=1}^{E} R_e^T A_e^{-1} R_e \underline{r} + R_0^T A_0^{-1} R_0 \underline{r}$$

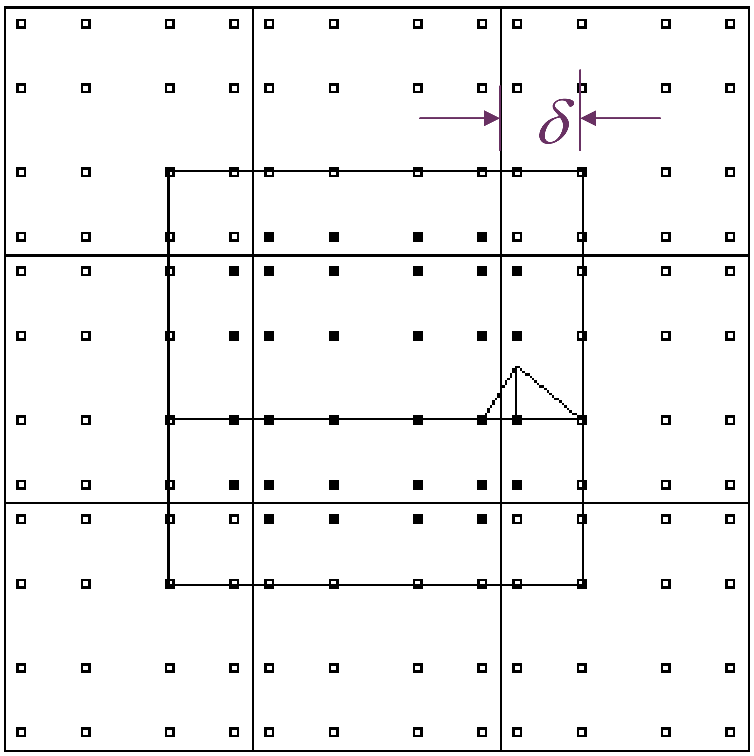

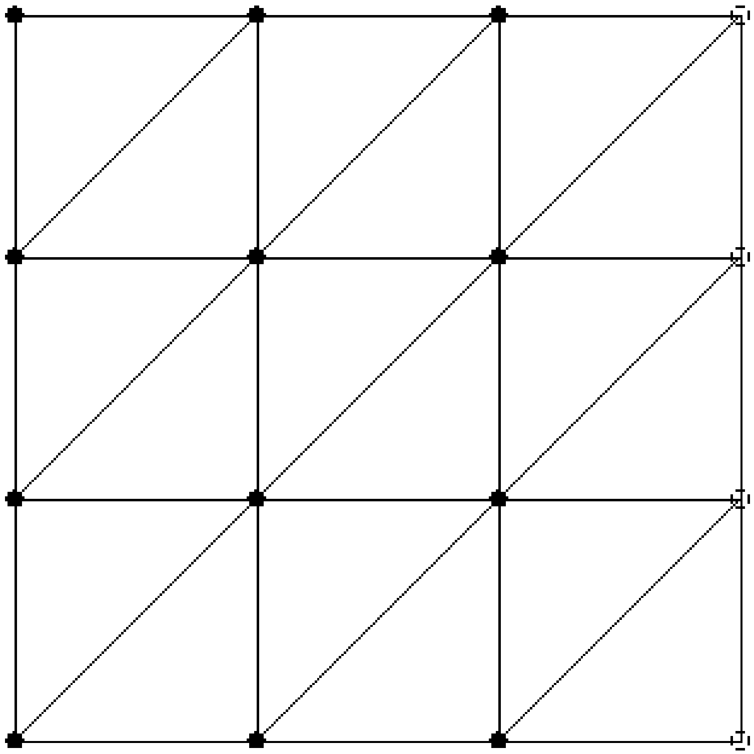

***Local Overlapping Solves**: FEM-based Poisson problems with homogeneous Dirichlet boundary conditions, A_e .*

***Coarse Grid Solve**: Poisson problem using linear finite elements on entire spectral element mesh, A_0 (GLOBAL).*

SEMG: Overlapping Additive Schwarz Smoother

- $M_{\text{Schwarz}} = \sum R_e^T A_e^{-1} R_e$ *Dryja & Widlund 87,...*
- Fast tensor-product solvers for A_e^{-1} *Rice et al. '64, Couzy '95*
- Bypasses cell aspect-ratio problem

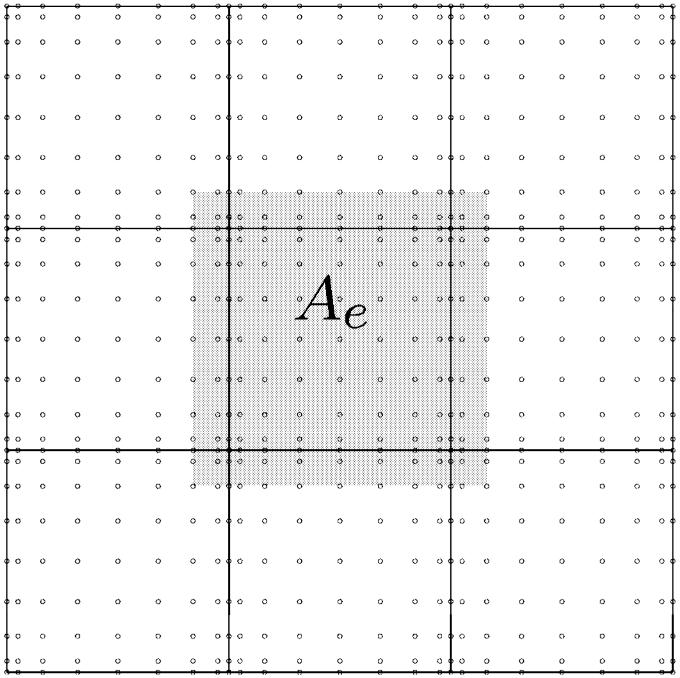

$$A_e^{-1} = (S \otimes S)\,(I \otimes \Lambda_x + \Lambda_y \otimes I)^{-1}\,(S \otimes S)^T$$

Importance of edge weighting

Lottes & F 04

- *Error after a single Schwarz smoothing step*

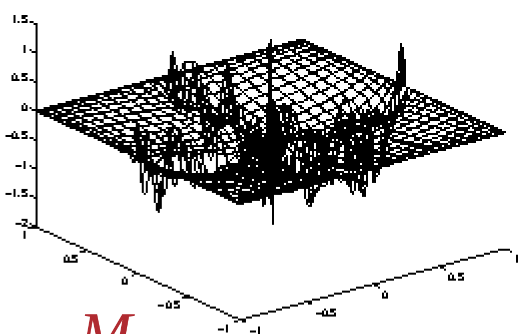

$M_{Schwarz}$

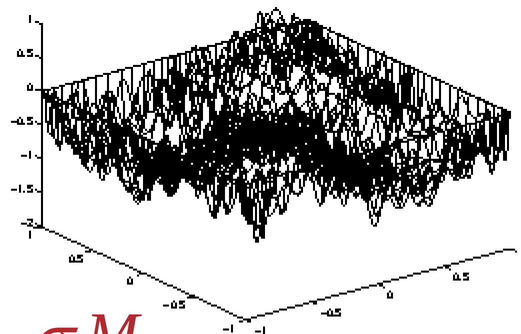

$\sigma M_{Schwarz}$

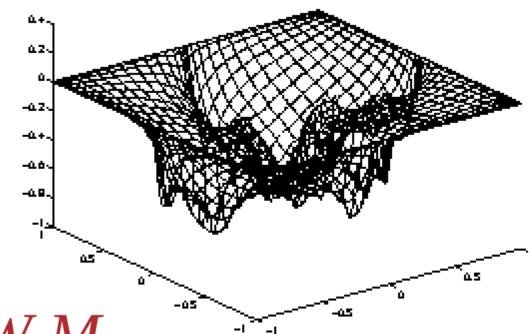

$W M_{Schwarz}$

- *Error after coarse-grid correction*

(2.0)

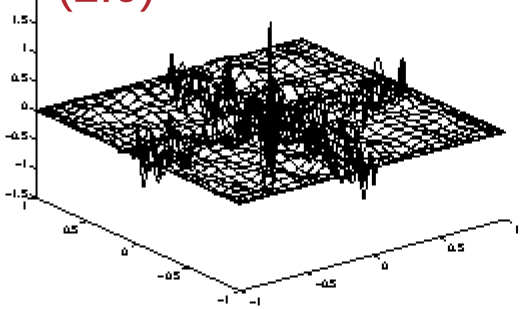

(0.8)

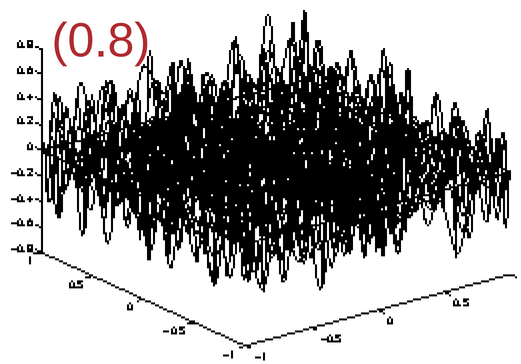

(0.15)

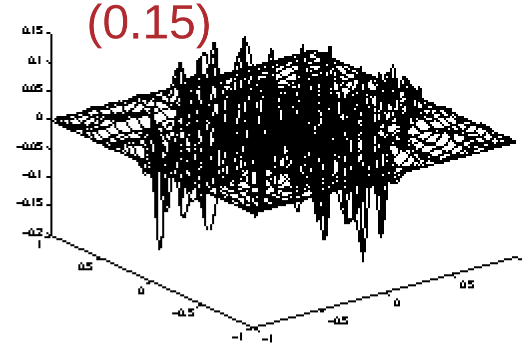

- *Weighting the additive-Schwarz step is essential* *(Szyld has recent analysis)*

3D Unsteady Navier-Stokes Examples ~10^6 dofs

- Hybrid Schwarz/MG: *F. & Lottes 05*
  - twice as fast as std. 2-level additive Schwarz
  - more robust in the presence of high-aspect ratio cells

Iteration count vs. timestep

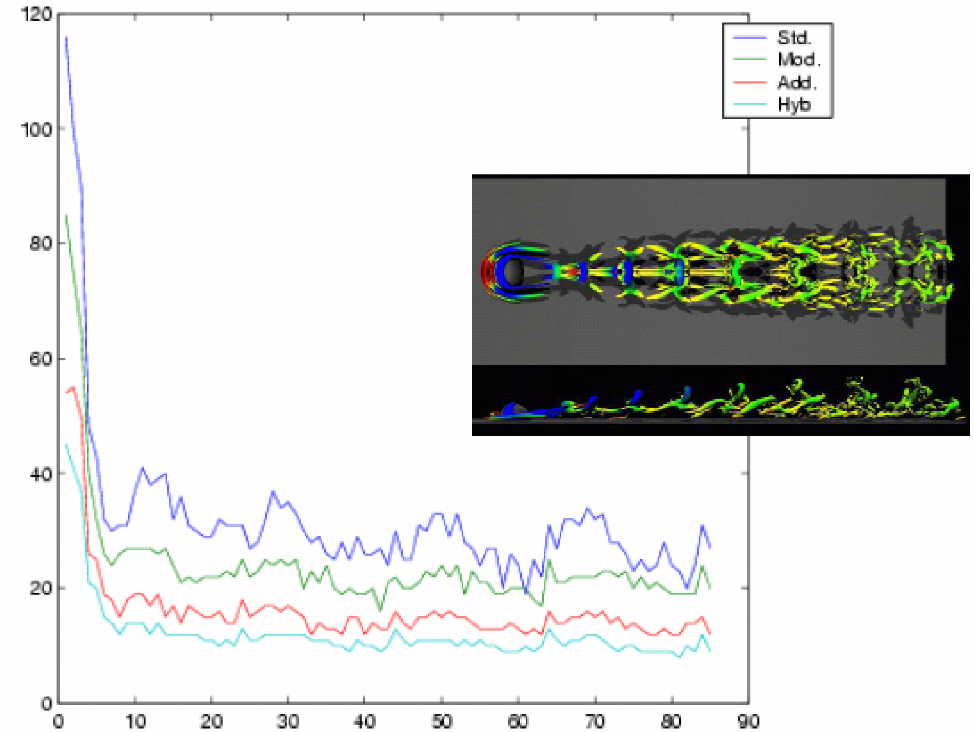

iteration count vs. timestep

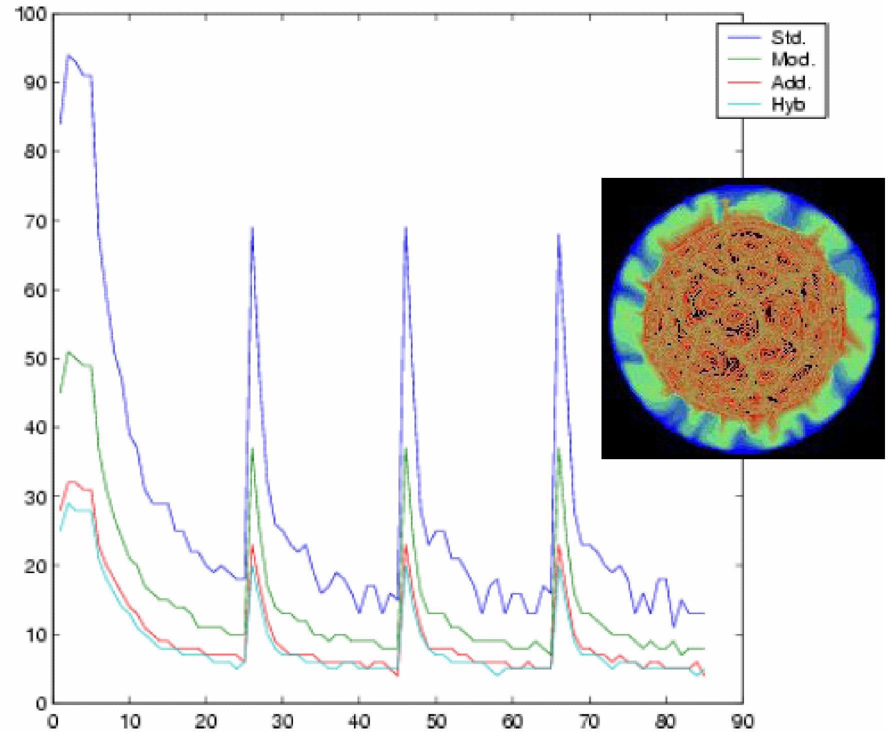

F. & Lottes 05

Scalability: Nek5000 on P=32K

Magneto-rotational instability (Obabko, Cattaneo & F.)

- *External science application on BGW:*
  - *E=140000, N=9 (n = 112 M)*
  - *P=32768*
  - *~ 1.2 sec/step*
  - *~ 8 iterations / step for U & B*
  - *Speed up of 1.96 for P=16K → 32K*

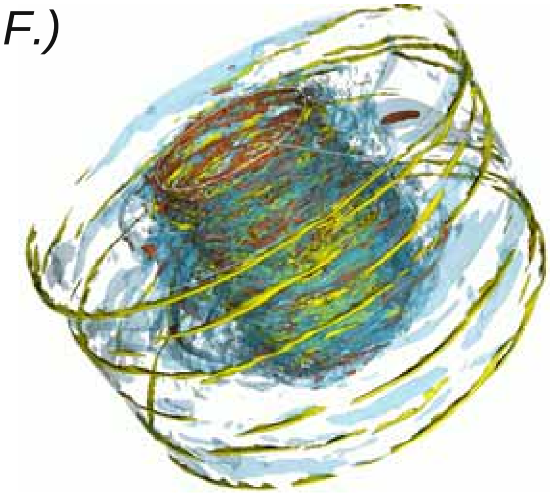

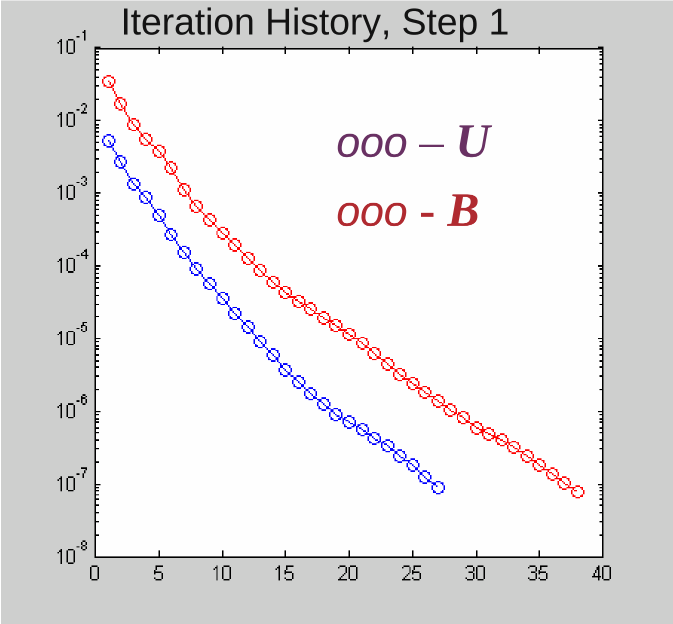

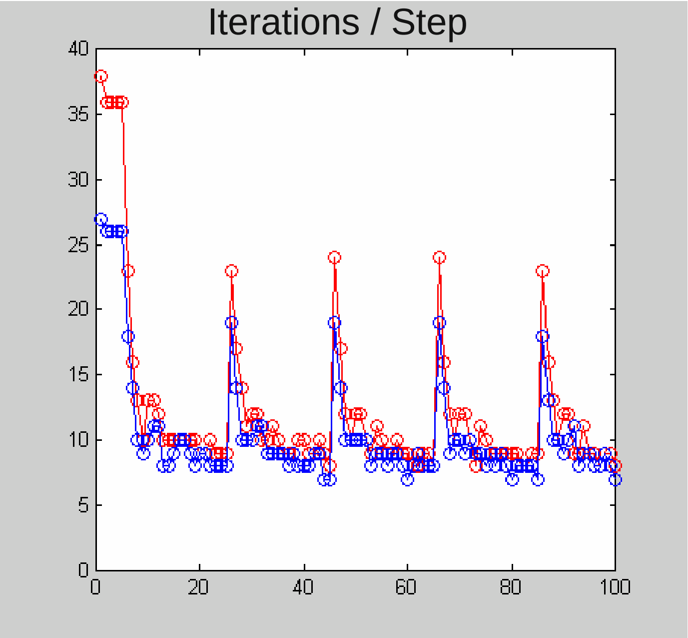

Vascular Flow Simulations

NIH w/ Loth & Bassiouny (UIC / UC)

Seeking to understand hemodynamics & vascular disease

- turbulence in AV grafts associated w/ graft failure *(Fillinger 93, Loth et al. 03)*
- understanding why/how transition occurs can lead to improved designs
- *also* provides an excellent opportunity for validation

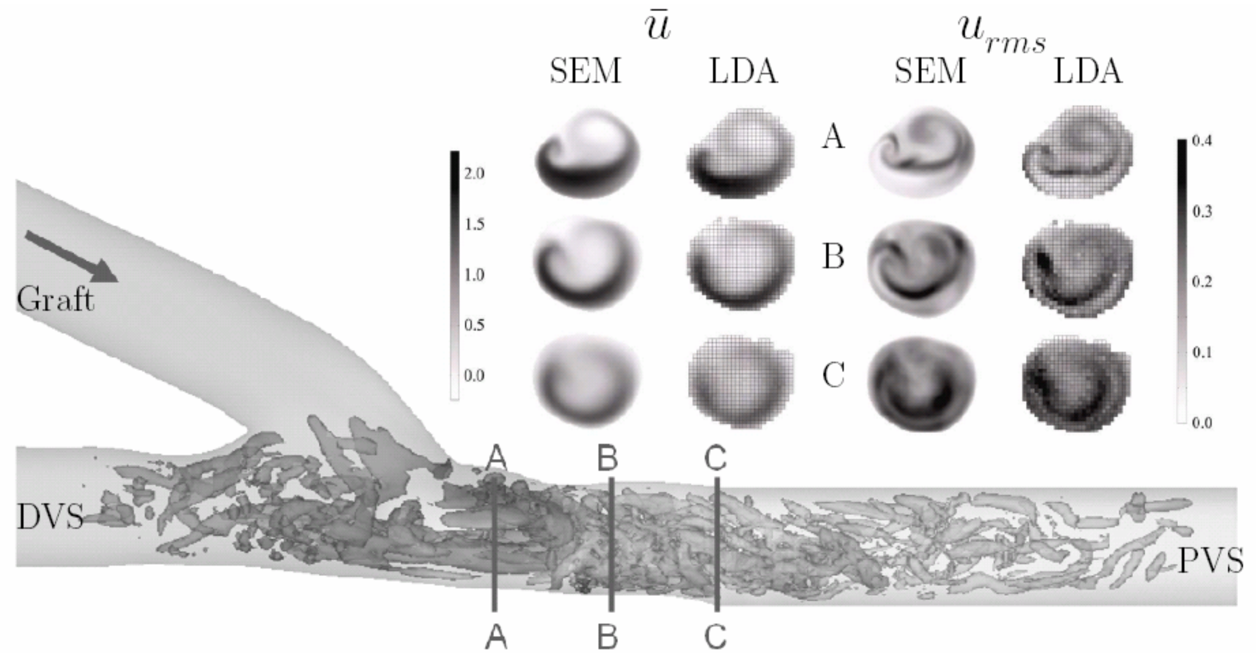

Coherent structures in AV graft at Re=1200; λ_2 criterion of Jeong & Hussein (JFM95)

Subassembly analysis of wire wrap fuel pins

Interchannel cross-flow is principal convective transport mechanism

- Uniformity of temperature controls peak power output
- A better understanding of flow distribution (interior, edge, corner) will lead to improved designs and design tools

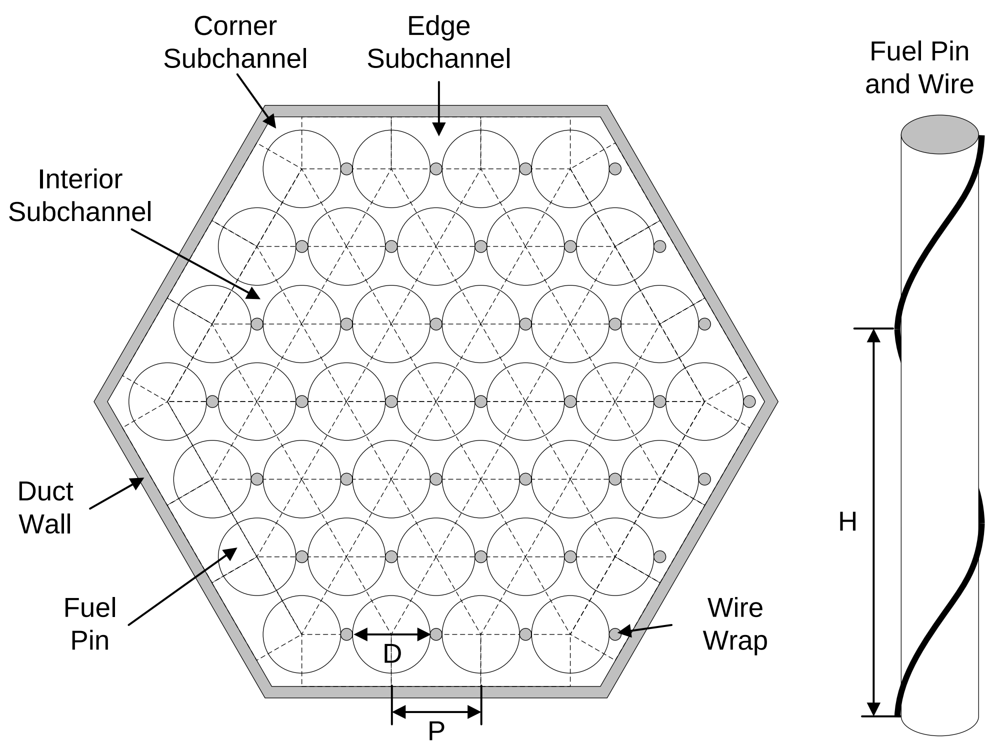

Preliminary analysis of wire-wrapped fuel pins

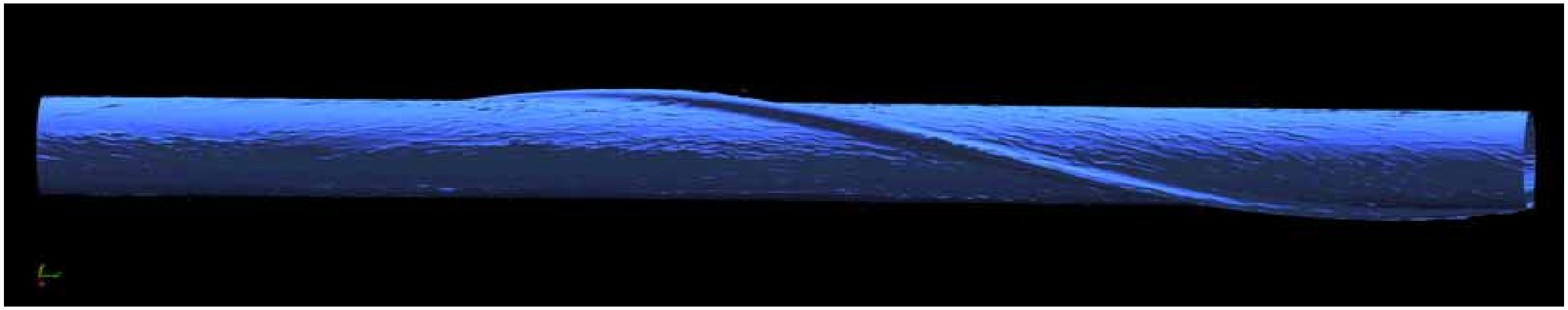

- Single pin in a periodic array:
  - Spectral element computation
  - Re=20000, 8.7 M gridpoints, 5 hours on P=2048 of IBM BG/L
  - Predicts interchannel velocity distributions in a large bundle system
- 7-pin configuration currently under study

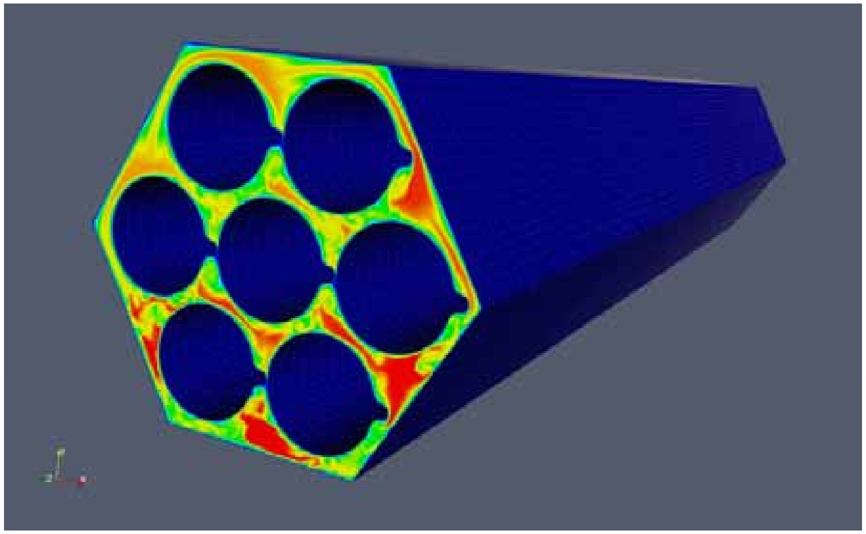

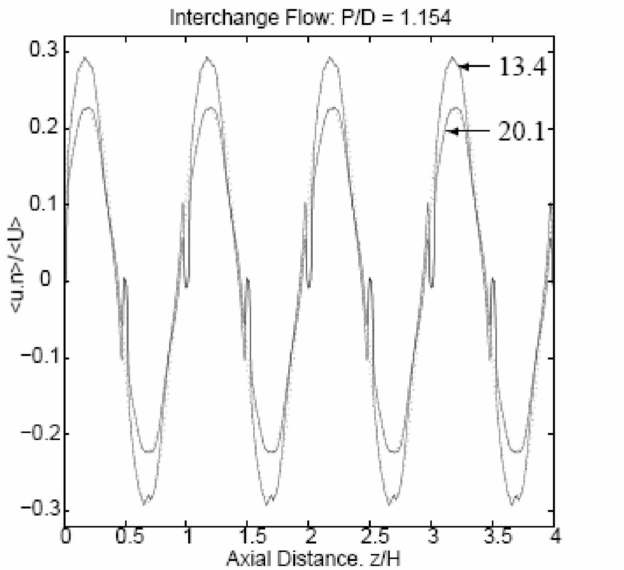

Concluding Remarks

- P = 100K is certainly within reach (and on the horizon in 08)
- P = 10^6 should be tractable, with care
  - *multigrid might be only solution for coarse-grid solves at this scale*
- Robust high-order methods
  - can be effectively applied in a variety of engineering and science applications
  - offer the potential to efficiently span a broad range of scales
- Many of the techniques described here can be extended to simplices.

Magneto-Rotational Instabilities

w/ Fausto Cattaneo (ANL/UC) and Aleks Obabko (UC)

- Spectral element discretization of MHD Taylor-Couette flow
  - *similar to expt. configuration of Goodman & Ji (PPPL)*

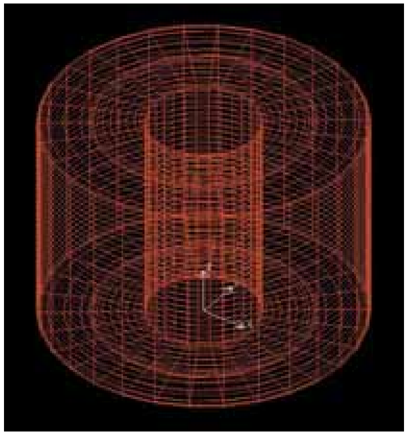

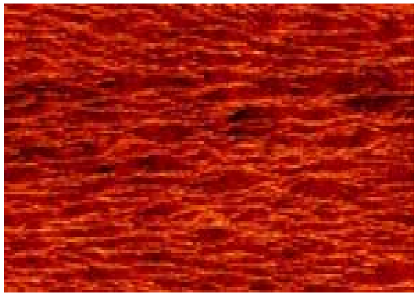

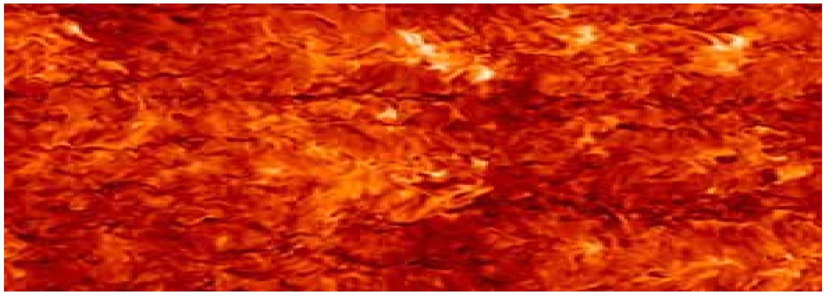

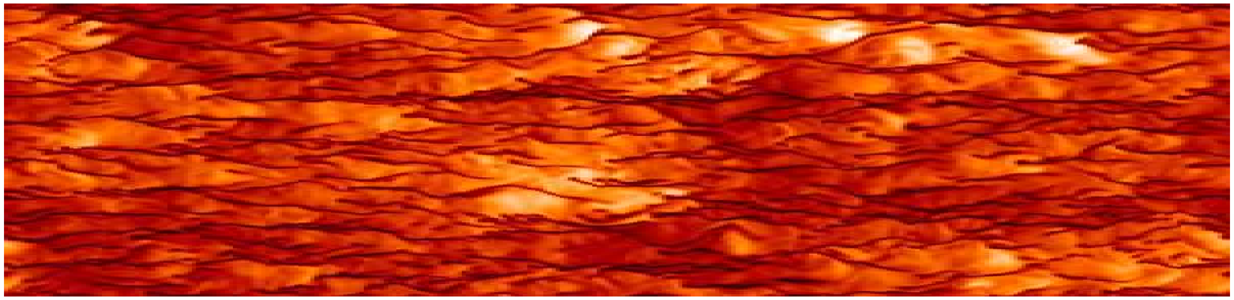

•Distributions of turbulent angular momentum transport at inner, mid, and outer radii

•Computations using 16K & 32K processors on BGW

•Predicts:
- ***MRI***
- ***sustained dynamo***

Filtering permits Re$_{\delta 99}$ > 700 for transitional boundary layer calculations

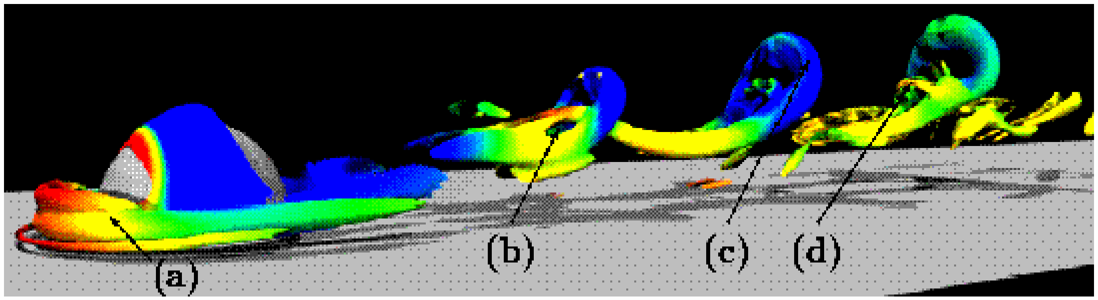

Figure 1: Principal vortex structures identified by $\lambda_2 = -1$ isosurfaces at $Re_k = 760$: standing horseshoe vortex (a), interlaced tails (b), hairpin head (c), and bridge (d). Colors indicate pressure. (K=1021, $N = 15$).

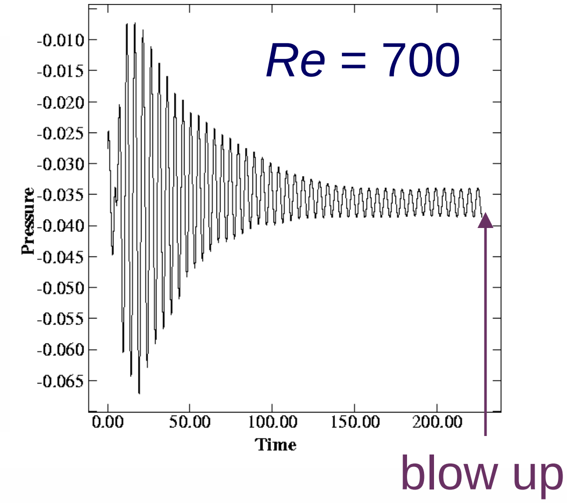

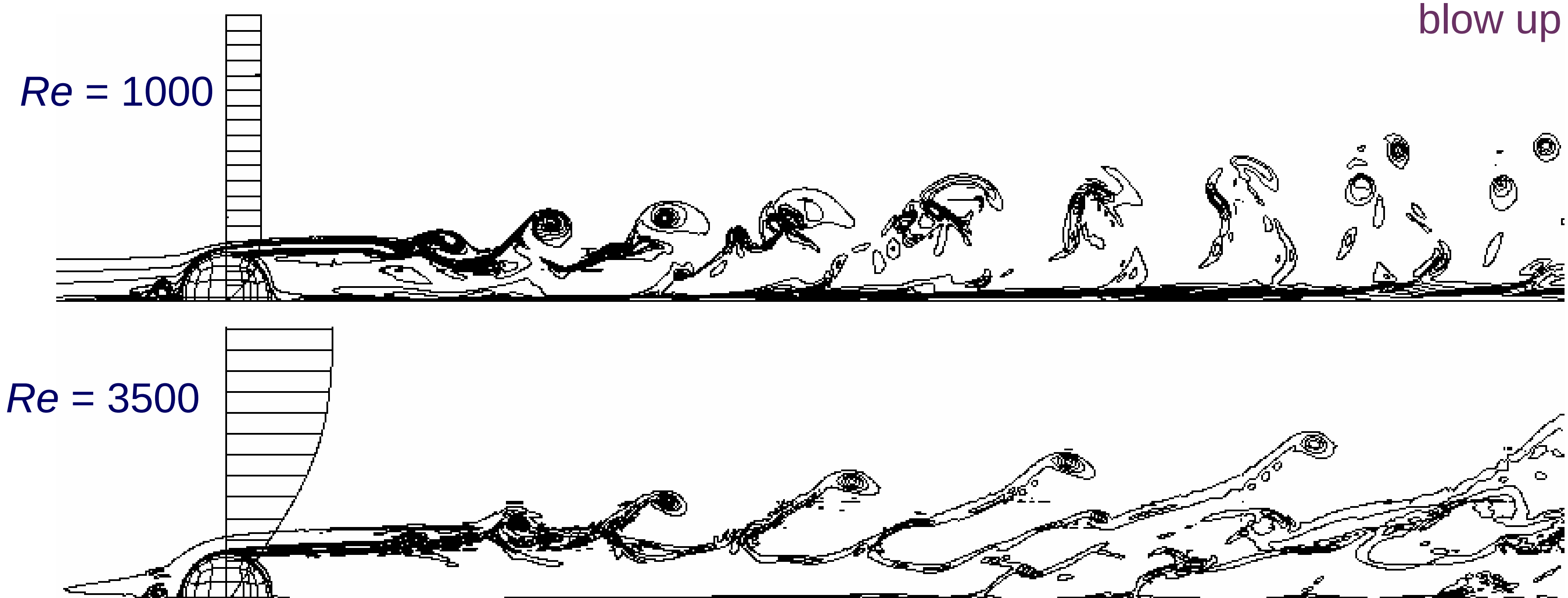

High Anisotropy Favors High-Order Methods

Anisotropy in fusion applications, model problem:

$$\frac{\partial T}{\partial t} - \nabla \cdot \mathbf{K} \cdot \nabla T = f \qquad \text{in } \Omega,$$

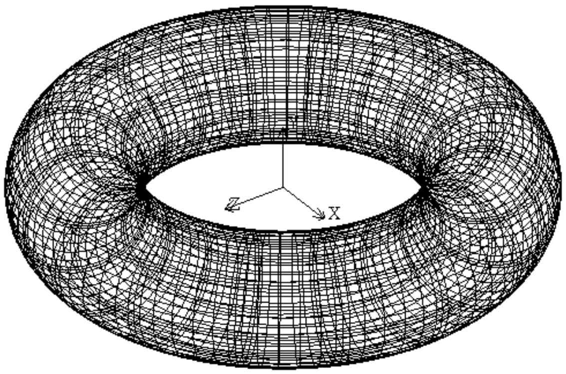

$$\mathbf{K} = \kappa_{||} \mathbf{b} \mathbf{b}^T + \kappa_{\perp} \mathcal{I}$$

$$\kappa_{||} / \kappa_{\perp} \approx 10^9$$

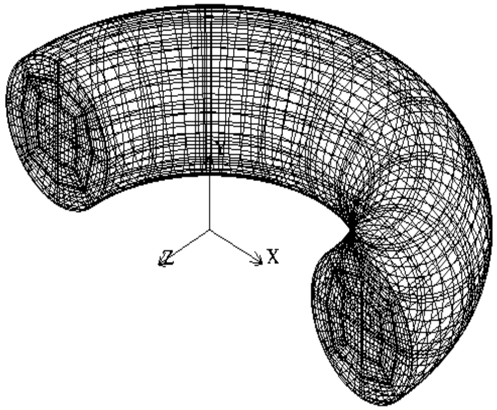

•**b** – normalized ***B***-field, helically wrapped on toroidal surfaces

•thermal flux follows **b**.

High degree of anisotropy creates significant challenges

- For $\kappa_{||}/\kappa_{\perp} \gg 1,$ this problem is more like a (difficult) hyperbolic problem than straightforward diffusion.
- $A = \kappa_{||} A_{||} + A_I$
- A_I controls *radial* diffusion
  - $A_{||}$ *must be accurately represented when* $\kappa_{||} >> 1$
  - *Error must scale as* $\sim 1 / \kappa_{||}$

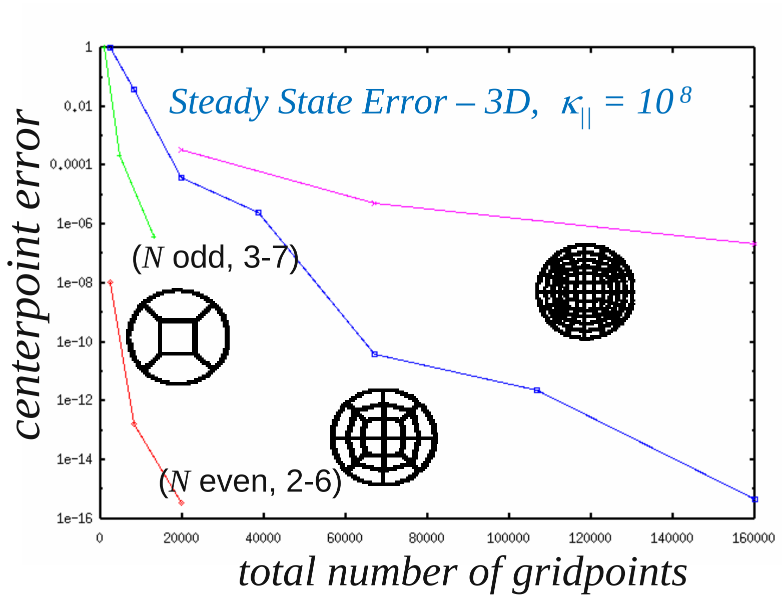

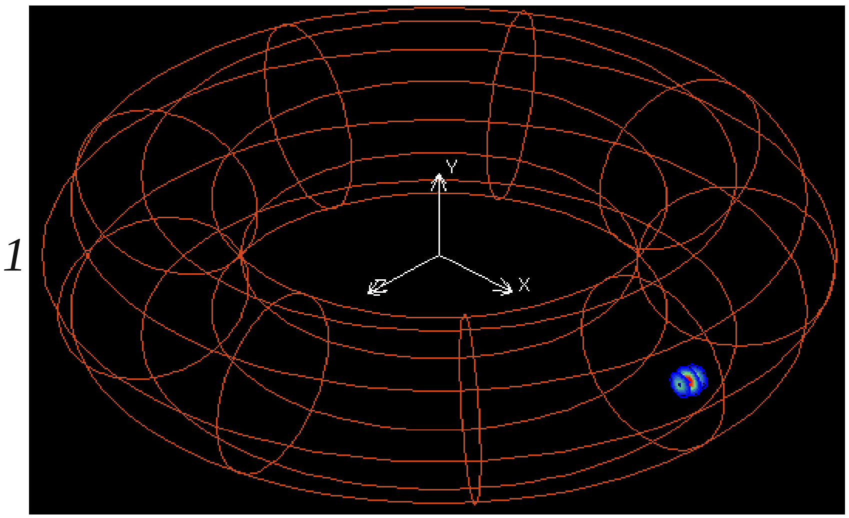

Significant advances enabled through DOE Applied Mathematics Program

- Stabilization for spectral element methods
  - Filtering
  - Dealiasing
  - Most significant advance in SEM since its development
  - Has enabled simulation of convection dominated flows that were previously inaccessible

- Spectral element multigrid J. Lottes
  - Most significant advance in SEMG in 15 years
  - First practical SEMG method

Heat Transfer in an fcc Lattice of Spheres at Re$_D$ *= 30,000*

E=1536 elements of order *N=14*

10 hours on 64 nodes for 1 flow-through time

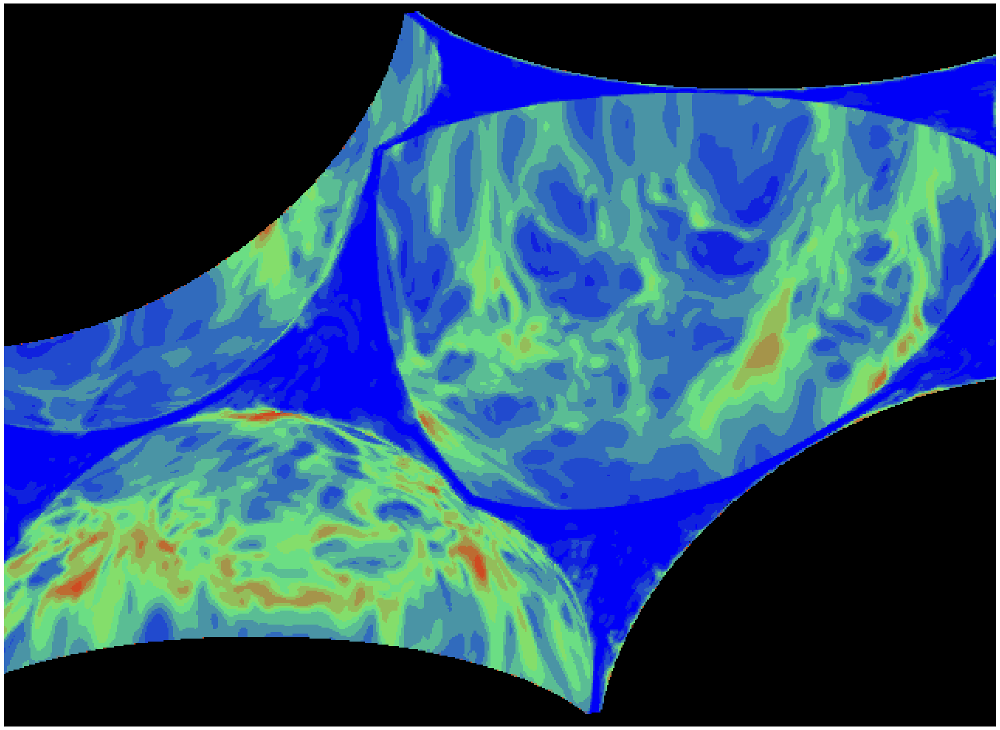

void-centric view

sphere-centric view

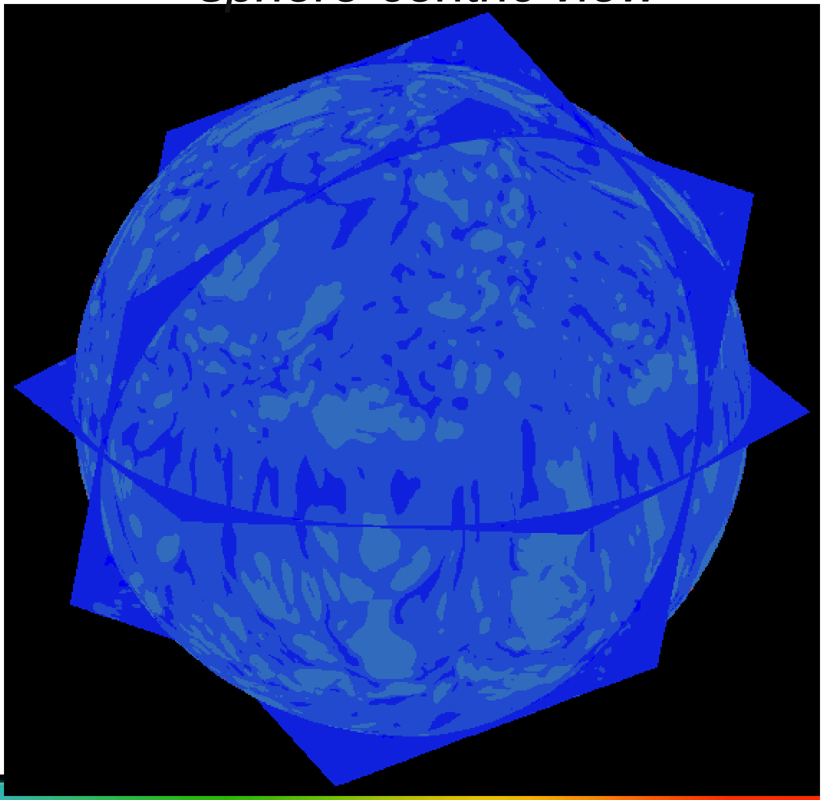

Max temperature fluctuation:
~ 14 x mean temperature change.

MRI & Origins of Accretion Disks

Cattaneo & Obabko

- **Accretion onto a central compact object is believed to power some of the most energetic phenomena in the universe**

- **If angular momentum is conserved, matter just orbits the central object**
  - ***Accretion rate is determined by the <u>outward</u> transport of angular momentum***
  - ***Frictional or viscous transport too inefficient to explain observed luminosities***
  - ***Something many orders of magnitude more efficient is needed***

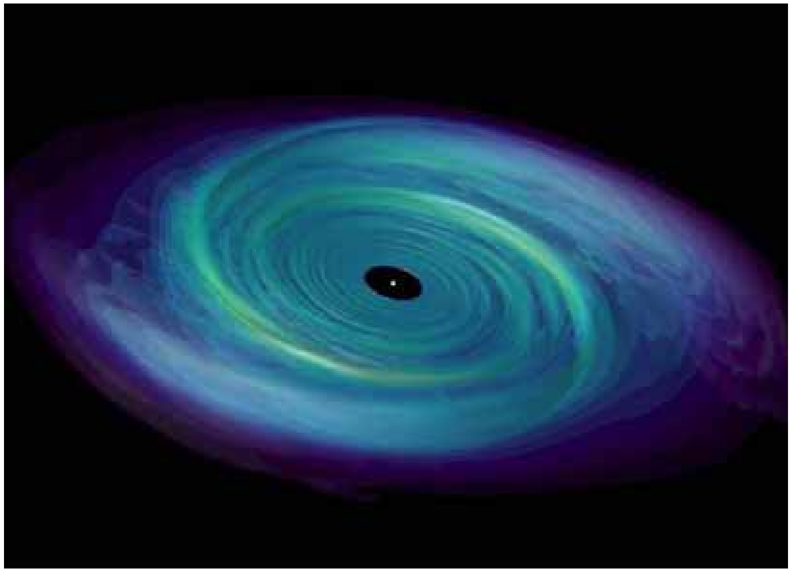

- **Turbulence has been suggested as momentum transport mechanism**
  - ***Yields reasonable disk structures and accretion rates***
  - ***Most astrophysical disks are Rayleigh stable***
  - ***What is the physical origin of the turbulence?***

Can we scale to P > 100,000 ?

- Robust performance estimates for various Poisson solvers:
  - Jacobi iteration scales, *but will not scale algorithmically*
  - The inner-products for conjugate gradient do not pose a significant difficulty, *on BGL*

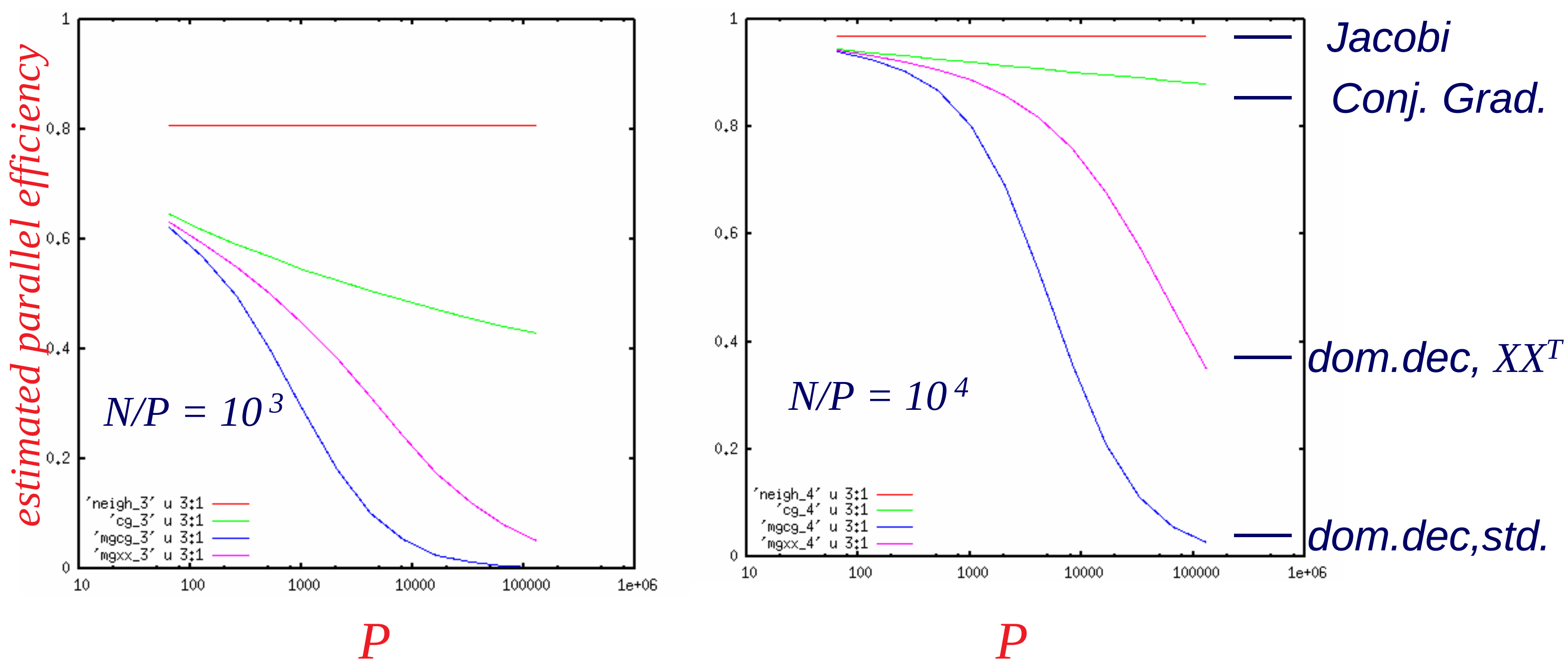

Example: SEM solution of turbulent MHD

- Scaling observations on BG/L and XT3, n=10.7 M

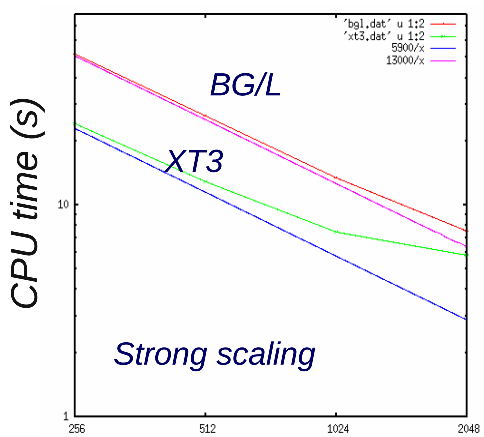

P

neigbor exch. time

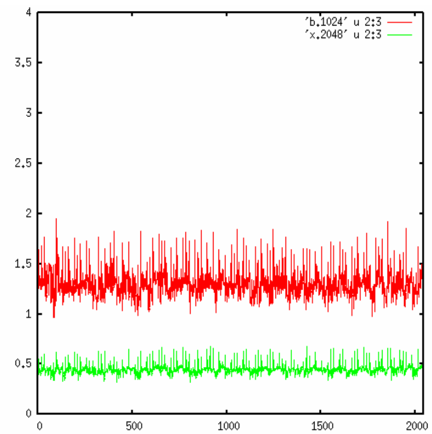

p = 1 … P

all_reduce time

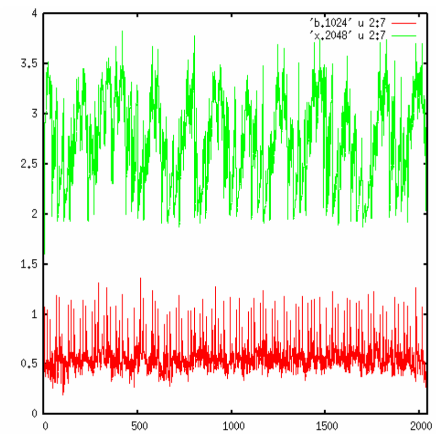

p = 1 … P

- Communication pattern is important only in small n/P limit.
- Currently running on P=32K BGL at Watson –
  - *No significant difficulties; efficiencies agree w/ model*
  - *Some software rewrite req'd – particularly wrt I/O (e.g., MPI-I/O)*

NEKCEM

Misun Min, MCS

SEM + DG for computational electromagnetics

- *Objective*
  - *Develop high-order EM code with significantly reduced PPW*

- *Target applications:*
  - *nanophotonics*
  - *accelerator design*
    - *long domain lengths*
    - *high accuracy required for post-processed analysis*
    - *Ideal for SEM*

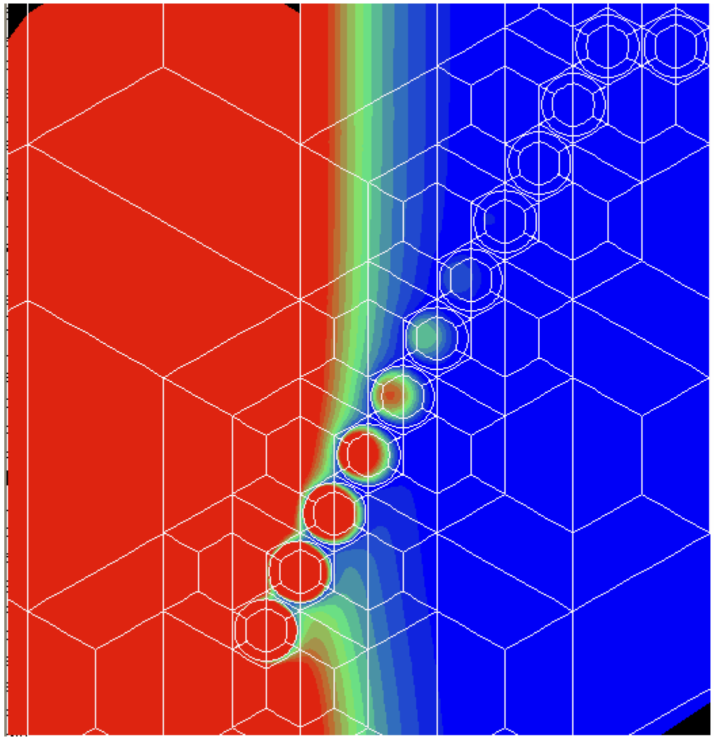

NEKCEM simulation of plane wave interacting with nanospheres

Accelerator applications

Misun Min, Y.C. Chae (APS)

- Wakefield computations for *psec* bunches require high accuracy and propagation of signals over long distances

- High-order methods offer a potential gridpoint reduction of 5x, *per space dimension*, for tera- and petascale applications of interest to accelerator designers

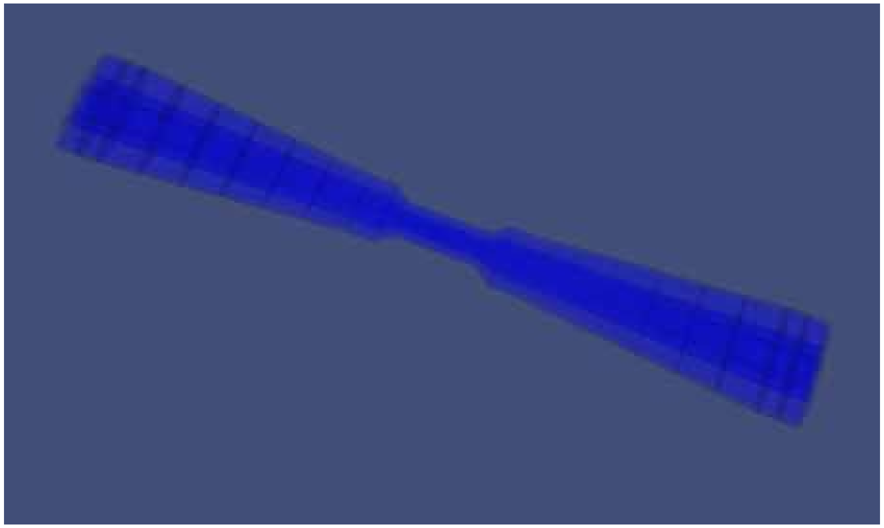

Spectral element mesh of APS beam chamber

Performance of SEDG Approach

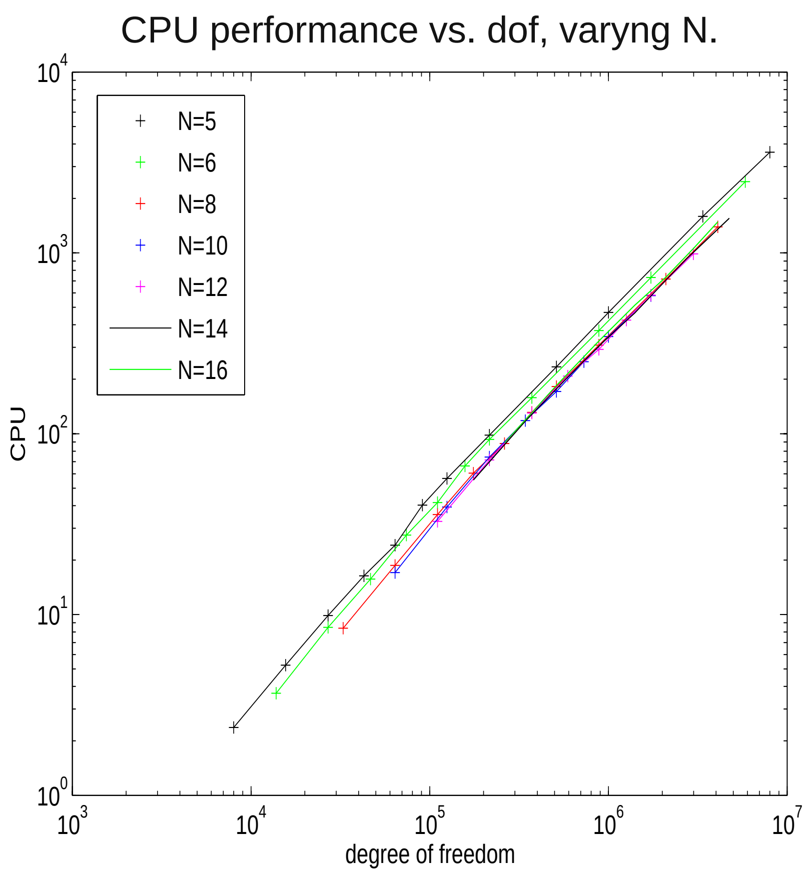

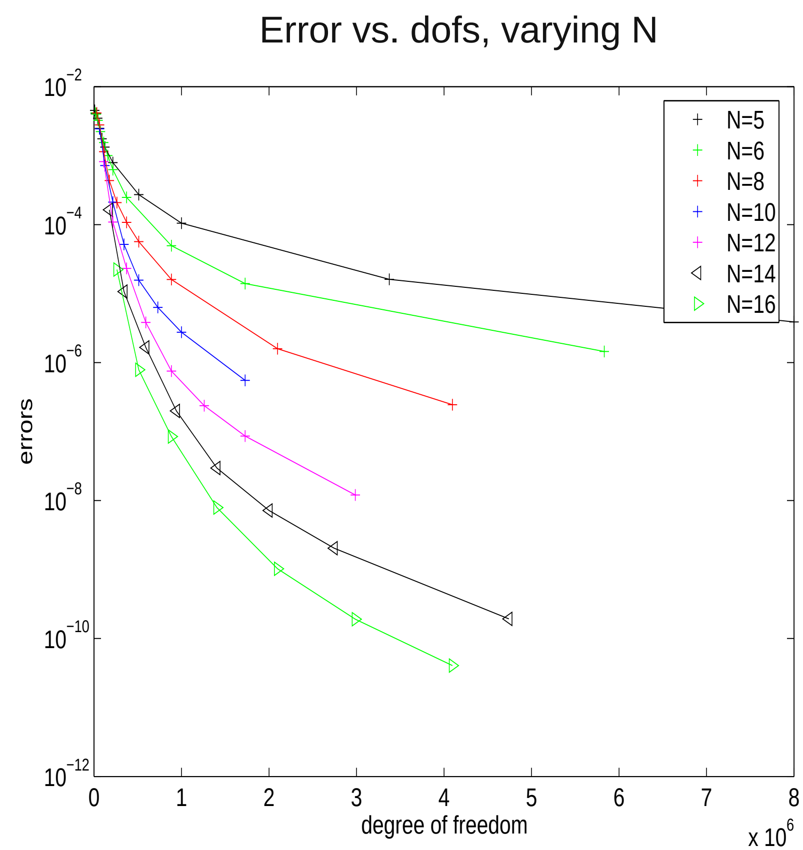

Periodic Box; 32 nodes, each with a 2.4 GHz Pentium Xeon

Reactor thermal hydraulics

- Key element of GNEP is to recycle spent fuel
  - reduce geological repository requirements by 100-fold
- Unlike LWRs, recycling reactors are not industry standard
  - *major design and safety regulation effort required*
  - *Petascale computing is a major advantage for the U.S. over competing nations, who in many cases have more current expertise*
  - *Reactor design software is ~ 30 years old – new software development effort is called for to reflect advances in algorithms and architectures*
- Thermal hydraulics for recycling reactors is governed by single-phase weakly compressible turbulent flow:
  - *LES, RANS, subchannel modeling will be principal analytical tools*
- *Ideal application for Nek5000*

Thermal Hydraulic Basics: core coolant problem

- Liquid metal coolant, pumped through the core consisting of hundreds of *subassemblies*:
  - Closed hexagonal canisters, open at top and bottom.
  - Contain 217 fuel pins, .8 cm diameter, in a hexagonal array.
  - Coolant passes vertically through *subchannels* (2 per pin) within subassembly
  - Fuel pins are separated by spacers and fluid can pass between subchannels

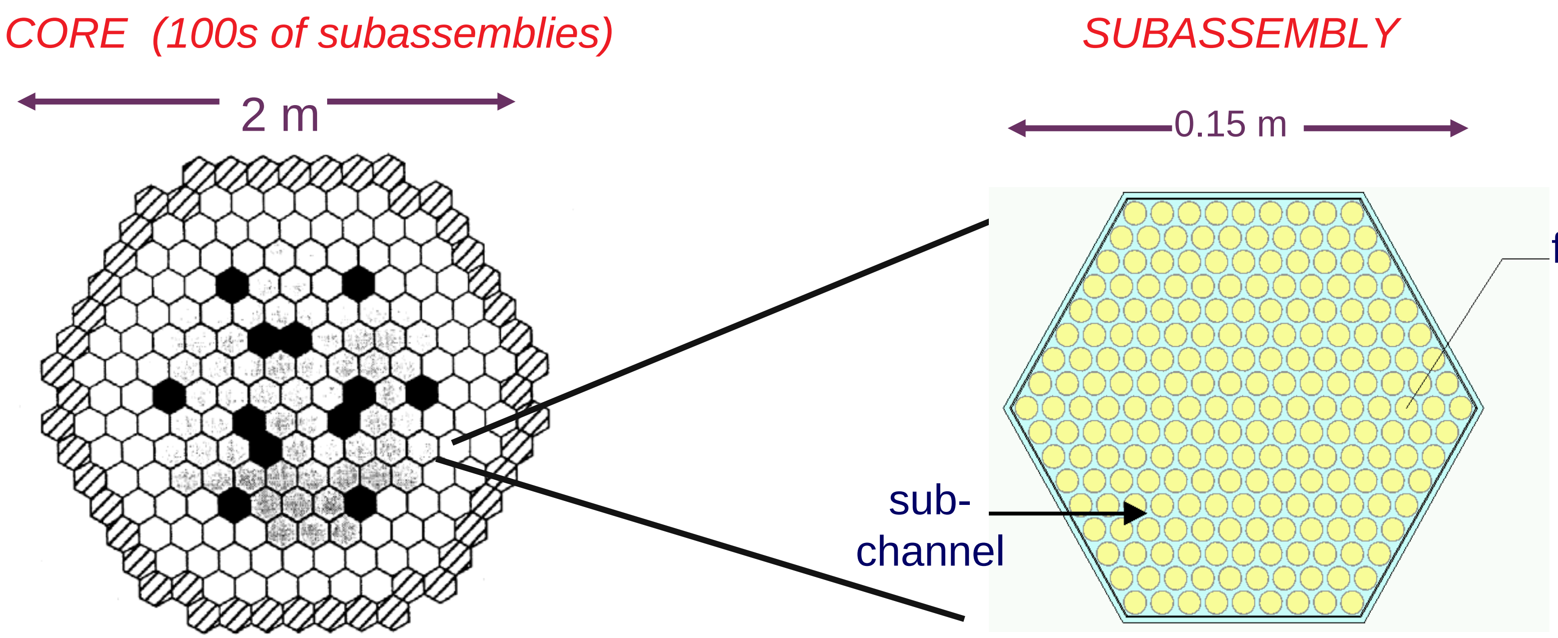

University Projects / Collaborators

- Provides excellent opportunities for
  - detailed validation
  - extension of physics
  - new features
- Active projects:
  - Transition in vascular flows
    - *Loth and Bassiouny (UIC, UC,* NIH funded*)*
  - Gravity currents in oceanic overflows
    - *Ozgokmen, Iliescu, Duan (U. Miami, V. Tech., IIT;* NSF funded*)*
  - Fundamental forces in particulate flows
    - *Balachandar, Najjar, Restrepo, Leaf (U. Fla., UIUC, U. Az., ANL)*
  - Others:
    - *Combustion (ETH), spatiotemporal chaos (Caltech), stenotic flows (Purdue),…*

Ongoing / Future Developments

- Aim:
  - Ensure that our high-order-based research codes are in a position to solve challenging DOE problems ranging from desktop to Petaflop.

- Algorithmic efforts:
  - Fast spectral semi-Lagrangian methods
  - Solvers / software scaling to $P > 10^6$
  - Fully-implicit DIRK schemes
  - Performance-optimized high-order HOMs for hybrid meshes
    - *tet, prism, hex*
  - DG methods for fluids / CEM

- DOE focus application areas
  - Fast reactor thermalhydraulics (DNS/LES/RANS/…)
  - Incompressible MHD *Cattaneo*
  - Accelerator/nanophotonics modeling *Min*
  - Liquid metal simulations (fusion applications) *Hassanein*

Extension to 2D

Nodal bases on the Gauss-Lobatto-Legendre points:

$$u(x,y) = \sum_{i=0}^{N}\sum_{j=0}^{N} u_{ij} h_i(x) h_j(y), \qquad h_i(\xi_p) = \delta_{ip}, \quad h_i \in \mathbb{P}_N$$

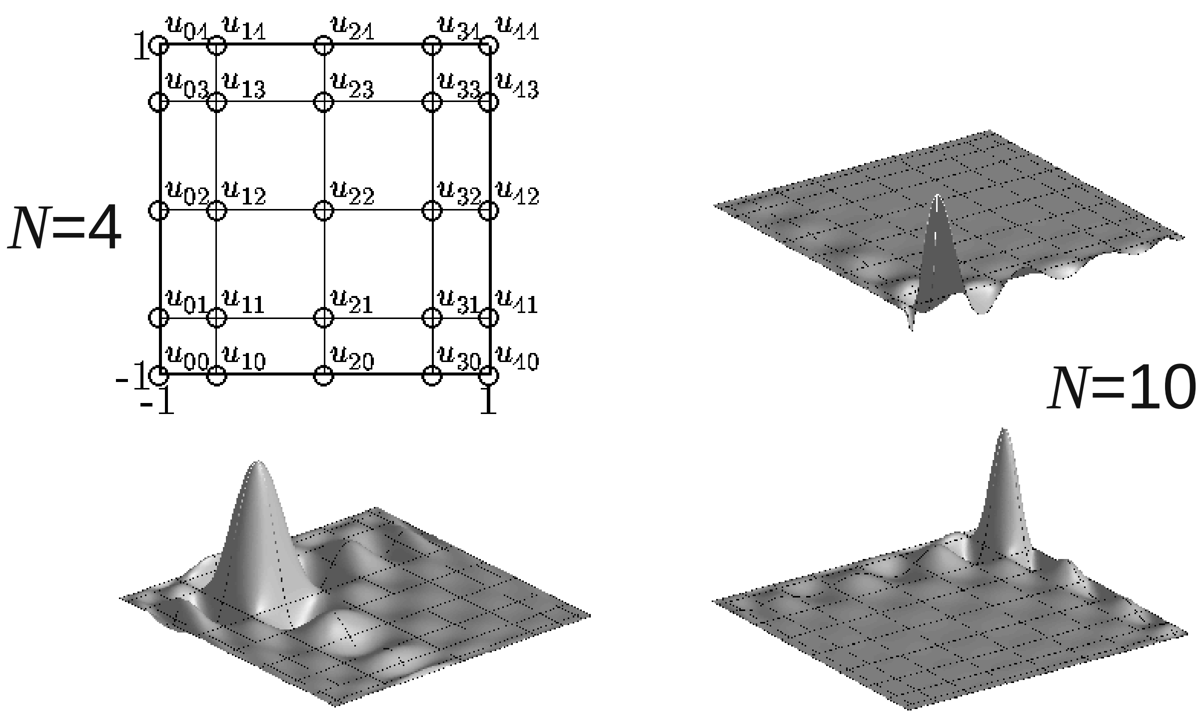

Matrix-Matrix Based Derivative Evaluation

- *Local tensor-product form* (2D),

$$u(r,s) = \sum_{i=0}^{N} \sum_{j=0}^{N} u_{ij} h_i(r) h_j(s), \qquad h_i(\xi_p) = \delta_{ip}, \ h_i \in \mathbf{P}_N$$

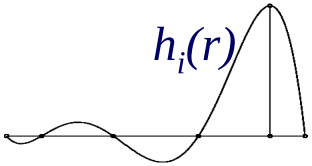

allows derivatives to be evaluated as matrix-matrix products:

$$\left.\frac{\partial u}{\partial r}\right|_{\xi_i,\xi_j} = \sum_{p=0}^{N} u_{pj} \left.\frac{dh_p}{dr}\right|_{\xi_i} = \sum_{p} \underbrace{\hat{D}_{ip} u_{pj}}_{mxm} =: D_r \underline{u}$$